

Review

Direct air capture multiscale modelling: From capture material optimization to process simulations

Dana Marinič^{a,b}, Blaž Likozar^{a,b,*}

^a Department of Catalysis and Chemical Reaction Engineering, National Institute of Chemistry, Hajdrihova 19, 1000, Ljubljana, Slovenia

^b Faculty of Chemistry and Chemical Engineering, University of Maribor, Smetanova Ulica 17, 2000, Maribor, Slovenia



ARTICLE INFO

Handling Editor: Jin-Kuk Kim

Keywords:

Direct air capture (DAC)
Thermodynamic isotherm model
Multiscale modelling simulations
Density functional theory (DFT)
Monte Carlo (MC)
Computational fluid dynamics (CFD)

ABSTRACT

A potential to decarbonize atmosphere, while simultaneously providing a feedstock for functional industrial applications, induces a strong economic incentive for direct air capture (DAC). However, DAC systems, developed to date, are energy, resource, and cost prohibitive. Measurement-complementing multiscale modelling has proven to be of a large visible value for the sorbent rapid screening from a vast scientific collection of prospective selected candidates, machine learning (ML) integration, and for the process design engineering with a characteristic low penalty for CO₂ regeneration and optimal uptake rates. The review provides an extensive evaluation of recent advances in multiscale modelling of DAC research. It introduces the theoretical physical descriptions of DAC, presents atom scale structuring, and brings together the state of the art of this, until now, poorly-researched analysis topic. Reviewed (CO₂ mass) transfer works span from the *ab initio* density functional theory (DFT) calculation relationships to mesoscale Monte Carlo, molecular dynamics simulations and micro-kinetics, adsorption/desorption, and lastly, most commonly-investigated specific macroscale concept. The modelled DAC processes properties reported in the literature have been compared, which allowed us to identify the most effective sorbents. Amine functionalized metal-organic frameworks exhibit low energy requirements, the lowest reported was 1000 kWh tCO₂⁻¹, while the lowest published cost was 60 \$ tCO₂⁻¹. Recently, there are progressively emerging promising new entrants into the DAC field, providing climate-neutral feedstock for commercial processes. The market demand for CO₂ is expected to exponentially rise up to 6.1 Gt in 2050, while the cost of implementing DAC technologies is predicted to be reduced under 125 \$ tCO₂⁻¹ in the year 2030. Further modelling research activities in CO₂ (sorption) bed form phenomena could not only break the barriers of current renewable technologies, but also couple the CO₂ reactions with the sequestration, reactors, and neutralization of harmful environmental pollutants, monoxide, NO_x, SO_x, etc. DAC could be ultimately coupled with electrolysis (hydrogen), producing e-fuels.

1. Introduction

The post-industrial upward trend in atmospheric carbon dioxide levels have led to its highest concentrations in roughly three million years (Sandalow et al., 2018) and have nearly doubled since the pre-industrial area (Bos et al., 2020). CO₂ is considered as the primary greenhouse gas; hence its removal has become one of the major global climate strategies. In 1999, Lackner et al. (1999) presented direct air capture (DAC) as one of the carbon dioxide removal (CDR) routes. The most elaborated techniques use the binding of CO₂ to liquid solvents or solid sorbents, which are covered in depth in several review studies (Sanz-Pérez et al., 2016) and briefly summarized in Supplementary

information. Today around 10,000 tons of CO₂ are removed per year thanks to this breakthrough technology (McQueen et al., 2021). However, this is merely a drop in the ocean compared to the 100–1000 gigatons of net CO₂ removal required by the end of this century in order to meet the indicative 1.5 °C target of the Paris Agreement (Wicaksana, 2016).

DAC is an emerging technology with great potential for mitigating climate change but also for providing feedstock for commercial processes. The global CO₂ demand analysis forecasted its increased need from 0.6 in 2030 to 6.1 Gt in 2050 due to the high production of renewable e-fuels and chemicals as a part of defossilisation process, assuming DAC to take a crucial part in the supply chain (Galimova et al.,

* Corresponding author. Department of Catalysis and Chemical Reaction Engineering, National Institute of Chemistry, Hajdrihova 19, 1000, Ljubljana, Slovenia.
E-mail address: blaz.likozar@ki.si (B. Likozar).

2022). The CO₂ prices are improbable to meet the DAC cost due to its extremely high energy requirement. The liquid and solid DAC systems require up to 10 and 8 GJ tCO₂⁻¹ respectively (Ozkan et al., 2022), in comparison with 3.5 GJ tCO₂⁻¹ for post combustion capture (Van Straelen and Geuzebroek, 2011). To reach the economic viability, the DAC cost needs to fall under 100 \$ tCO₂⁻¹ (Ozkan et al., 2022), as in 2022 the DAC cost was set between 125 and 350 \$ tCO₂⁻¹ for a large-scale plant (International Energy Agency, 2022). Luckily, multiscale modelling shed light on the system behaviour and adsorption process, providing us valuable guidelines for process design engineering with a characteristic low penalty for CO₂ regeneration. Successful implementation of DAC modelling could result in potential cost savings and revenue generation.

Despite the growing interest in this field, there is a lack of comprehensive multiscale models. Experimental approach methodology is already immensely applied with the derived representative expressions of the CO₂ flow in concentrated gas streams. However, these effective models cannot be directly translated to DAC due to the (minute) ambient CO₂ partial pressure for absorption (Yang et al., 2020). Several different CO₂ capture review articles exist in the literature; nonetheless, they are all focused on the carbon capture from concentrated gas streams or DAC sorbents analysis. This review paper provides a comprehensive evaluation of recent advances in multiscale modelling of DAC research. It also aims to address knowledge gaps in nano, meso, and macroscale modelling, since several modelling techniques, like CFD, remain elusive. We identified a number of serious deficiencies in the presented computational techniques, such as the neglect of the enhancing or diminishing water effect on CO₂ isotherms. The modelled DAC processes properties reported in the literature have been compared, exposing the best performances presented so far.

2. Why is direct air capture commercialization limited?

After a successful capture, CO₂ can be stored in deep geological formations (Deschamps et al., 2022) or it can become an important industrial resource, especially in the chemical and transport sector (Breyer et al., 2019). IEA stated that in 2022 only 18 DAC plants were operating worldwide, capturing more than 0.01 MtCO₂ y⁻¹ (International Energy Agency, 2022). The three pioneer companies, namely Carbon Engineering (Canada), Climeworks (Switzerland), and Global Thermostat (USA), are paving the way for DAC technology development since 2009 (Table S1). Recently, there are progressively emerging promising new entrants into the DAC field (Table S2), which is highly desired and necessary due to the scale of the problem. However, very little information on many of them is publicly available.

DAC is still in an early stage of commercial development since it is considered to be technically challenging, energy-intensive and one of the most expensive CDR routes, consuming up to three times more energy than other CDR pathways (Sandalow et al., 2018). Although the energy is derived from renewable sources such as geothermal energy, it is noteworthy that several companies continue to depend on natural gas. Therefore, the availability of inexpensive energies is entirely determining the fate of DAC. As the financial sustainability of many technologies is strongly dependent on the violent fluctuation of fossil fuel price, the oil unfortunately still plays a crucial role in economic stability (Vochozka et al., 2020). However, every commercialization is limited in its infancy. A techno-economic assessment of DAC predicted a fair reduction of DAC price to 50 € tCO₂⁻¹ by 2040 (Fasihi et al., 2019). For example, biochar's ability to recover other critical raw material, especially phosphorous, can make certain carbon sequestration technologies financially viable (Maroušek and Gavurová, 2022).

The main reason for high energy demand lies in the low CO₂ concentration in the atmosphere, which is 0.04% compared to 5% in natural gas-fired flue gas and 12% in coal-fired flue gas (Sandalow et al., 2018). The energy requirement highly depends on the enthalpy of the solvent/sorbents-CO₂ binding reaction. Strong CO₂ binding to adsorbent is

desired in terms of selectivity, however, it increases regeneration cost because of the high energy required for the CO₂-adsorbent interaction fracture. On the other hand, the low enthalpy of adsorption is desired for easier regeneration but is accompanied with low selectivity, which means other molecules such as water are also attached to the material (Bernini et al., 2015).

Transitioning to a low-carbon economy does not eliminate the need for carbon sources, as the abundance of materials we consume continues to rise. The only sustainable carbon sources are from biomass or directly from air. Biomass is dispersed in nature, recalcitrant, its composition varies, shows difficulties in its conversion and is already vastly studied. Getting carbon from the atmosphere, though diluted, seems like a far future reality. As a society, it is imperative that we recognize the value of renewable carbon and DAC due to its potential to address some of the world's most pressing social challenges, including climate change, economic development and environmental justice. But most importantly it is raising imperative ethical and policy questions that need to be addressed. The DAC recognition and acceptance are growing which can also attribute to its higher demand. The growth of carbon markets also induces a strong development incentive for DAC (Guo et al., 2022).

3. Multiscale modelling

Multiscale modelling emerged as a promising tool for rapid screening from a vast scientific collection of prospective selected candidates. It was also proven to be a convenient alternative to laboratory work since it gives insight into a complex system otherwise difficult to explore experimentally. Furthermore, computational power has reached levels, which allow to simulate and analyse every aspect of DAC design, considerably reducing the time and cost of upgrading or developing new carbon capture technologies (Huš et al., 2019; Miller et al., 2014).

Direct air capture is a multiscale heat and mass transfer process and cannot be wholly described only by one modelling technique (Wang et al., 2018). Therefore, several modelling methods on nano, meso, and macroscale have been applied for a thorough survey of DAC and are summarized in Table 1 and visually presented in Fig. 1.

First principle quantum mechanics methods, such as density functional theory (DFT) calculations, describe the adsorption behaviour on nanoscale, identify binding mechanism (Huš et al., 2019), active sites for CO₂ capturing, easily accessible positions for oxidation (Buijs, 2019a), calculate binding energies, and analyse pore size distribution (Zhu et al., 2021b). DFT-obtained interaction energies can be fitted to applicable potential function, also called Force Field (FF). FF surveys the intermolecular interactions between adsorbates or adsorbate and adsorbent. It can be also empirically obtained, but yields less accurate gas uptakes (Xiang et al., 2010). FF parameters serve as input values for Monte Carlo (MC) simulations which predict the statistics-based properties of systems on a longer length scale. Molecular dynamic (MD) simulations often complement MC to describe the dynamic properties of the system (Xiang et al., 2010) or for mechanism validation (H. H. Wang et al., 2020). Radial density functions are used, which compute the probability of finding an atom at a specific distance (Yang et al., 2020). By inputting the MC results into the saturation adsorption isotherm model, the macroscopic adsorption properties can be predicted. However, due to the lack of modelling results, simple mathematical isotherm models are usually applied by fitting the thermogravimetric analysis (TGA) uptake experimental data. Equilibrium adsorption capacity obtained by the isotherm model serves as an input in linear driving force (LDF) models, which evaluate the rate of adsorption and describe the transport phenomena in the interface and particle interior. They are also the key element in dynamic or process models, which predict the heat and mass transfer on the exterior of the sorbent particle (Wang et al., 2018). Moving forward from sorbent to DAC process design, macroscopic CFD simulations describe the idealized flow in air contactor, predict pressure drops, and compare different geometries and types of structures (Ryan et al., 2013). The main purpose of the applied modelling is to design

Table 1

An overview of different modelling techniques at different length scales used for efficient DAC process description. By combining two or more techniques multiscale models can be obtained, which describe the process more accurately.

Scale	Modelling technique	Main outputs
nano	Density functional theory	<ul style="list-style-type: none"> energies of active species adsorption/binding energies distance of interactions identifying binding mechanisms identifying active sites for CO₂ capturing identifying easily accessible positions for oxidation pore size distribution
meso	Monte Carlo	<ul style="list-style-type: none"> average thermodynamic properties particle interactions and potential energies between two CO₂ molecules or CO₂ molecule with sorbent framework insight into the capture mechanism
	Molecular dynamics	<ul style="list-style-type: none"> dynamic properties radial density functions
macro	Isotherm models	<ul style="list-style-type: none"> the CO₂/H₂O equilibrium adsorption capacity on solid-phase
	LDF kinetic models Dynamic/process models	<ul style="list-style-type: none"> the CO₂ adsorption capacity against time energy requirement rate of CO₂ extraction and productivity working capacity (WC) total cost of the process concentration profile at the exit of the bed the fractional bed usage the overall CO₂ capture fraction the breakthrough time the adsorption rate constant
	Computational fluid dynamic	<ul style="list-style-type: none"> air flow characteristics pressure drops reactor shape sorbent loading heat transfer simulations

economically acceptable, practical, highly selective, and stable sorbent materials with a low energy penalty for CO₂ regeneration and a cost-effective system (Buijs, 2019b) to reach the stated goal of reduced cost below 100 \$ tCO₂⁻¹ (Valentine and Zoelle, 2022).

4. Density functional theory

DFT presents a favourable compromise between the cost and accuracy and is therefore an effective method for the calculation of the energies of active species and molecular geometry determination (Huš

et al., 2019). The computational depiction of the electronic effect has been used as the leading tool for the atomic/molecular-level grasp of CO₂-sorbent weak intramolecular forces or strong covalent bonds. Physisorption and chemisorption differ in adsorption energies, the first having the heat less and the latter more than 60 kJ mol⁻¹, although the energies may deviate in the case of zeolites (McQueen et al., 2021). Physical adsorbate may be acceptable for the post combustion capture, but the application in DAC is less reasonable due to the low selectivity since its performance is highly dependent on the CO₂ partial pressure (Lee et al., 2023). On the other hand, in order to bypass energy-intensive processes, physical adsorption is desired to be explored to a greater extent.

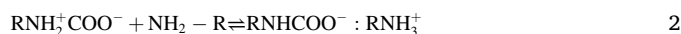
4.1. Amine-functionalized sorbents

The sorbent type selection is of high importance as it determines the overall system (Sandalow et al., 2018). Solid-supported amines are furthest along in development because of their high structure stability and high adsorption capacity even at low partial pressure of CO₂ and low regeneration temperature, which are one of the major drawbacks of currently applied sorbent materials (Bos et al., 2019; Deng et al., 2021). CO₂-selective amine groups (e.g. polyethylenimine) are functionalized on a highly porous support (e.g. zeolites, fumed silica, porous alumina supports, MOFs, nanocellulose, resins, activated carbon, carbon nanotubes, organic polymers, etc.) (Elfving et al., 2017a; McQueen et al., 2021) via impregnation, grafting, or in situ polymerization (Elfving and Sainio, 2021).

The CO₂ capture in amine-functionalized adsorbent occurs via zwitterion formation (Eq. (1)), which is stabilized by water as well as neighboring amines.



Under dry conditions the intermediate is subjected to deprotonation by a neighboring amine group and ammonium carbamate formation:



Anila and Suresh (2021) conducted an extensive study of the covalent and non-covalent interactions of the guanidine (G) molecule with CO₂ molecules. The theoretical results stated that the high adsorption capability is caused by the formation of the large cyclic clusters with zwitterion character (G⁺)-(CO₂⁻). The nature of the formation of optimized complexes is exothermic ($\Delta G_{(\text{G}-\text{CO}_2)_8} = -2602 \text{ kJ mol}^{-1}$) and the most stable cluster (G-CO₂)₈ had the interaction energy of CO₂ with imine atom in G of 115 kJ mol⁻¹.

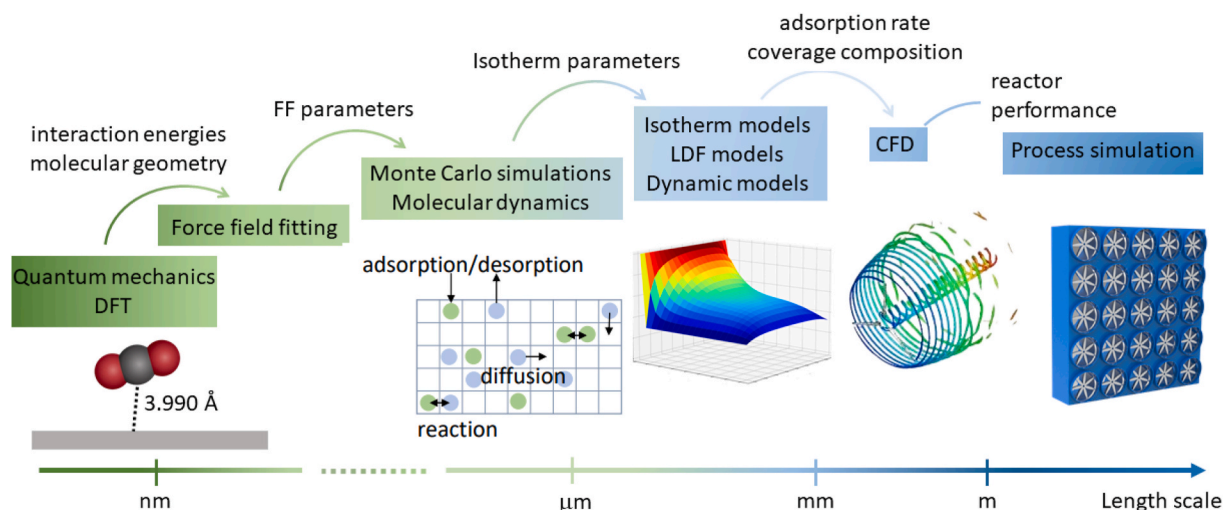


Fig. 1. Schematic representation of simulation methods at different length scales potentially used in a multiscale model and their outputs.

Humid conditions lead to several yet not extensively explored mechanisms, such as the formation of bicarbonate or hydronium carbamate (Elfving and Sainio, 2021). Several studies explored the carbamic formation via CO₂ adsorption onto amine-functionalized MOF (Planas et al., 2013), mesoporous silica (Afonso et al., 2019; Li et al., 2016), Lewatit VP OC 1065 (Buijs and De Flart, 2017), and the reaction of CO₂ with ammonia, MEA or DEA (Arstad et al., 2007). Numerous DFT cluster models of CO₂-amine adducts were applied for energetic analysis of the species, which determined the stability and the favoured species formation route (Afonso et al., 2019). Carbamic acid and carbamate moieties were found to be the most stable, highly depending on the hydrogen bonds formation. However, another DFT model study (Li et al., 2016) showed that the CO₂ capture mechanism in humid conditions most likely leads to hydronium carbamate formation. Two possible identified CO₂ capture pathways were direct amine-H₂O catalysis (in humid conditions) or amine catalyzed (in dry conditions) formation of carbamic acid (Buijs and De Flart, 2017).

DFT molecular simulations for Lewatit VP OC 1065 sorbent were reported by Buijs who conducted an extensive study on the CO₂ capturing process (Buijs and De Flart, 2017), deactivation mechanism by CO₂ (Buijs, 2019b), and oxidative deactivation (Buijs, 2019a). In the first study (Buijs and De Flart, 2017) the resin structural features, CO₂ adsorption mechanism, CO₂ and H₂O preferred mode of adsorption were evaluated. The amine groups were found to alternate in close vicinity, could react with each other, or enable CO₂ capture. The complexation enthalpies for CO₂ were -19.1 and -19.8 kJ mol⁻¹, in humid and dry conditions, respectively. The deviation of experimental CO₂ sorption data from the Langmuir model was in further research related to the loss of CO₂ uptake capacity due to the CO₂ and O₂ degradation effect on the sorbent upon prolonged exposure to high temperatures (70–120 °C) and high CO₂ pressure or air. In the study (Buijs, 2019b), a three-step deactivation process by CO₂ was investigated. Firstly, an amine group and CO₂ self-catalyze to carbamic acid. Further rate-determining step, acid decomposition to an isocyanate, is followed by benzyl amino group attachment to isocyanate and urea species formation, which are responsible for the CO₂ capacity loss. Moreover, easily accessible positions for oxidation and active sites for CO₂ capturing were identified (Buijs, 2019a). Oxidation starts with the physisorption of O₂ to the amino groups on the resin, which leads to the formation of α -amino-benzyl hydroperoxide. The lower physisorption energy of CO₂ with the resin (-19.5 kJ mol⁻¹) in comparison to O₂ (-4.5 kJ mol⁻¹) but lower CO₂ air concentration at room temperature leads to the equivalent occupation of the active sites with both molecules. The following thermal decomposition forms the corresponding amine and half-aminal, the latter solvolyses to aldehyde responsible for deactivation. Considering the input of E_a = 117.5 kJ mol⁻¹ for hydroperoxide formation and E_a = 120.0 kJ mol⁻¹ for its decomposition, the model predicts a 20% CO₂ capacity loss in 12 h at 80 °C.

Ionic liquids (IL) exhibit high uptake capacities and insignificant volatility. Nonetheless, their high viscosity augments mass transfer limitations, which were studied by CO₂ absorption and desorption experiments fitted to isotherms (Lee et al., 2020) and modelled by mass transfer correlations (Wilcox et al., 2014). Polymeric IL possess comparable synthetic flexibility and better stability (Erans et al., 2022). Atomistic modelling (Shi et al., 2018, 2020; Wang et al., 2017) explained the thermodynamic water influence on MSA-based DAC performance. Computationally optimized molecular structures provided insight into the interaction mechanism between water and different counteranions (CO₃²⁻ and HCO₃⁻). The carbonate ion was found to be less stable under dry conditions, leading to energetically favoured HCO₃⁻ and OH⁻ formation, which bind less water than CO₃²⁻. Hence more OH⁻ ions are available for CO₂ capture under dry conditions compared to wet (Shi et al., 2018, 2020). The spatial distribution of water molecules was shown to alter with ion type, from being evenly distributed around the carbonate anions to forming clusters around bicarbonate. During CO₂ adsorption the hydrophilicity of the polymeric IL decreases with anion

conversion from bicarbonate to carbonate and OH⁻, which releases the water, binds CO₂, and transfers the heat out of the sorbent, offering the sorbent cooling possibility (Wang et al., 2017).

Zhao et al. (2022) explored the performance of mixed metal oxides (MMOs) as support materials for TEPA-impregnated sorbents. The experimentally observed and DFT-interpreted oxygen vacancy defects on Mg–Al MMOs computationally explained the strong chemical interaction between MMO support and amine and enhanced stability. The defects can act as an electron acceptor, strongly bind the molecule, which results in outstanding regenerability due to the enhanced charge transfer. DFT studies also compared the MMOs and SiO₂ supports (Fig. 2).

4.2. Metal-organic framework

Open metal ions in the metal-organic framework (MOF) were identified as preferential adsorption sites for CO₂ through DFT combined with ¹³C NMR (Kong et al., 2012), neutron diffraction measurements (Wu et al., 2010), neutron powder diffraction experiments (Queen et al., 2011) and infrared and Raman spectroscopy (Dietzel et al., 2008). CO₂ binds to Mg²⁺ or Ni²⁺ sites through ion pair electron donation with end-on coordination, suggesting the physisorptive binding nature (Ding et al., 2019). Bien et al. (2020) studied the heterobimetallic MOFs containing nucleophilic transition metal (Cu, Co, Ni, and Zn) hydroxide functional groups at the Kuratowski-type metal nodes. The formation of intercluster hydrogen-bonding interactions leads to a strong CO₂ binding mechanism with Ni–OH, Co–OH, and Zn–OH and therefore higher affinity even at low pressure.

5. Monte Carlo simulations considering adsorptive and desorptive dynamics of CO₂

Statistical mechanism models, such as Monte Carlo (MC) models, are used to simulate the interactions and migration of a large number of particles and calculate the average thermodynamic properties. MC represents an effective alternative to classical mechanics and quantum mechanics, because it displaces the time-consuming calculations for each particular atom. The method is based on random configuration generation by molecular movement with an equal probability of translation, rotation, insertion, deletion, and random reinsertion. The exactly solved energy, pressure, and specific heat can be derived from modelled energy level distribution of the system (Coskuner, 2018).

Among frequently applied ensembles, grand canonical (GC) ensemble is extensively applied for molecular simulations in adsorption systems since it calculates the number of moles of molecules in the pore directly (Yun et al., 2002). It was demonstrated to efficiently simulate the adsorption isotherm (Xie et al., 2016) and to effectively predict the quantity of adsorbed material as a function of external conditions (Coskuner, 2018). Fitting the GCMC simulated isotherms to experimental isotherms one can obtain all Toth's isotherm parameters (Ji et al., 2022; Wang et al., 2018). However, the simulations of gas mixtures with low CO₂ concentrations lead to bad statistics and long runs are required for reasonable results (Chanajaree et al., 2019).

The study presented by Wang et al. (2018) is a perfect representation of multiscale modelling (Fig. 3). Periodic dispersion-corrected DFT was first used for the calculation of Lennard-Jones (J-L) parameters needed for J-L potential calculation. GCMC obtained final number of adsorbate molecules and potential energies between two CO₂ molecules or CO₂ molecule with sorbent framework were the main input values for the saturation adsorption amount calculation, which was further used for Toth's isotherm parameters calculation. With the help of the pseudo-first order LDF model, the concentration of each solute in the particle at any adsorption time and position were obtained. They combined microscale DFT, mesoscale GCMC method, and macroscale dynamic model to examine the heat and mass transfer process in an adsorbent bed filled with the 5A zeolite particles used as potential CO₂

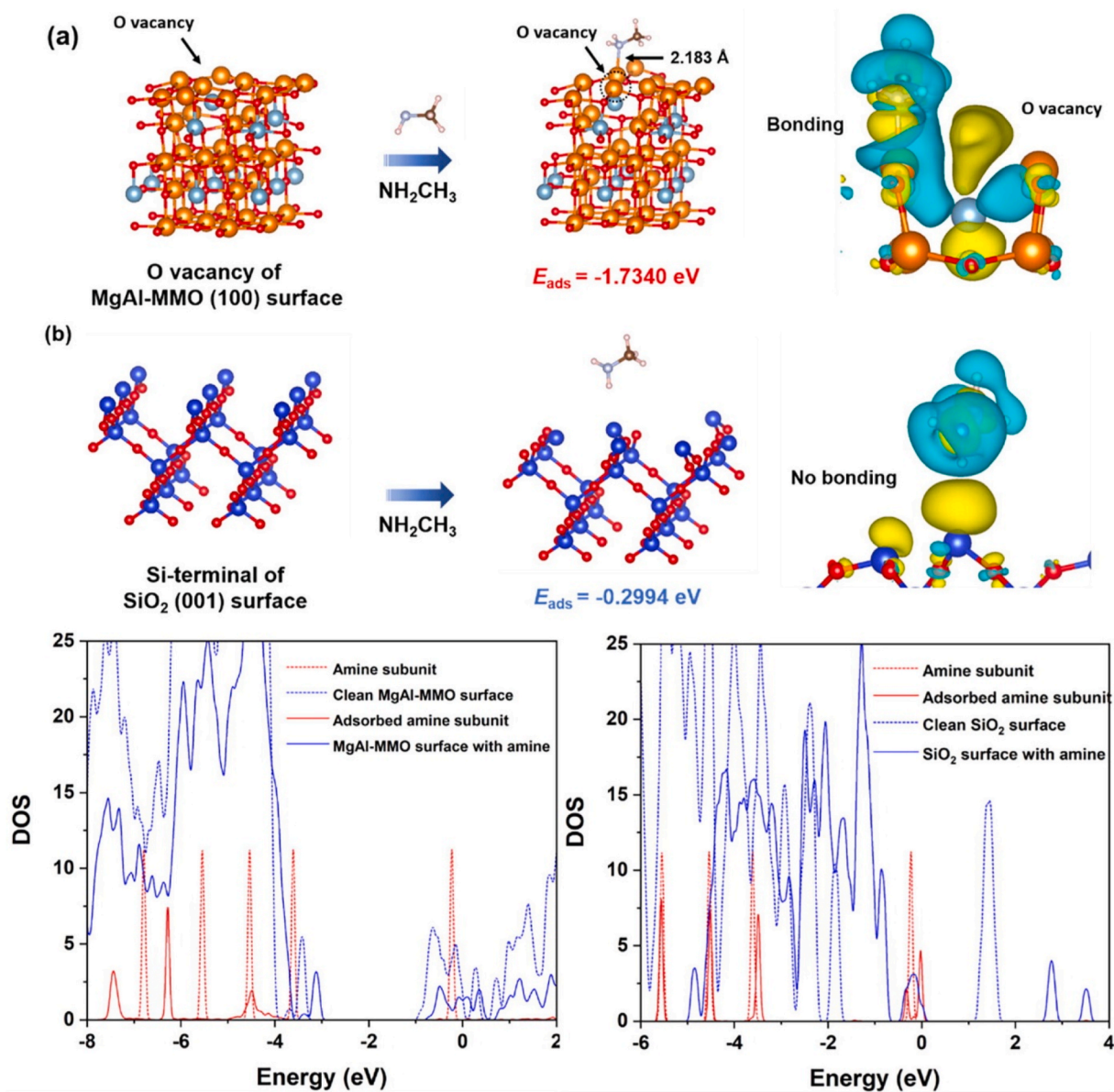


Fig. 2. DFT compared MMO and SiO₂ supports. The adsorption energy of amine subunit (CH₃NH₂) over a) oxygen vacancy of Mg–Al MMOs (100) surface (–1.73 eV) and b) SiO₂ (100) surface (–0.3 eV) indicated strong physisorption or weak chemisorption, c) density of states of Mg–Al MMOs and d) density of states of SiO₂ system. Reproduced with permission (Zhao et al., 2022). Copyright 2022 Elsevier.

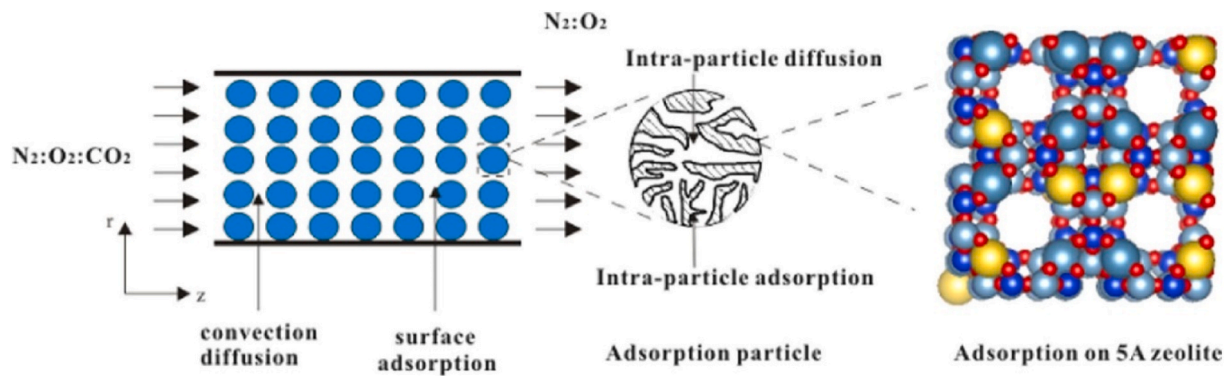


Fig. 3. The scheme for the multiscale simulation method of 5A zeolite, suggesting the interdependency between models on different length scale. Reproduced with permission (Wang et al., 2018). Copyright 2018 Elsevier.

space shuttle sorbents.

Chanajaree et al. (2019) investigated the diffusion of CO₂ and CH₄ in air mixture and preferred adsorption sites of gas molecules on the ZIF-78 framework by MD, while the adsorption was studied by Gibbs MC simulations. Adsorption techniques were found to be appropriate for CO₂ capture due to high CO₂ selectivity, while membranes and techniques based on permeation are also applicable for the separation of CH₄. The increased CO₂/N₂ selectivity and uptake capacity of the azo-linked nanoporous covalent organic polymers was computably explained by the generation of the N₂-phobic framework by azo groups (Patel et al., 2013).

MOFs were also studied by Bernini et al. (2015) who screened several hypothetical and real sorbents to obtain improved CPO-27-Mg composition with the optimal degree of ethylenediamine functionalization. Simulations evaluated 18 potential CPO-27-Mg structures with 15–100% functionalization degree of the coordinatively unsaturated sites. It was found that the initial structures with *gauche* conformations were energetically more stable compared to *trans* conformations. The CO₂ uptake was discovered to be affected by the chemical composition, pore shape, and available pore volume, but remarkably not by free void volume. The study concluded that the optimal structure was 50% functionalized CPO-27 composition. However, due to energy-intensive regeneration, the expanded CPO-27 structure based on a weaker Lewis acid metal ion was proposed as a more economical option.

An even more extensive MOF study (Deng et al., 2020) combined the canonical MC method, MD, and machine learning to screen 6013 ever reported computation-ready experimental MOFs. The adsorption and diffusion properties of the gases (CO₂, N₂, and O₂) when binding to MOFs were first determined by MC and MD. Univariate analysis was later used for relationship establishment between the adsorption and desorption selectivity. After adopting the finest algorithm by the multivariate analysis, 14 MOFs with optimal properties were screened out of 6013 potential MOFs. HIQPEE presented the largest diffusion selectivity (62.27 Å), while NORGOS had the largest adsorption selectivity but also the maximum heat of adsorption (51.67 kJ mol⁻¹). The best diffusion separation performance of a MOF was found to be when its pore-limiting diameter was similar to the CO₂ dynamic diameter.

Yang et al. (2020) studied the pressure fluctuation influence of the FF on the CO₂ adsorption loading on zeolite 13X. The found special mechanism of CO₂ adsorption present under low-pressure conditions once again proved the inapplicability of post-combustion CO₂ capture models, since the FF underestimate CO₂ adsorption loading at low pressures. MD revealed microstructures of the host-guest interactions, the established mechanism helped to predict a more accurate FF and isotherms. Faujasite with a low Si/Al ratio was further studied (Yang et al., 2021a) due to its improved adsorption capacity, which was attributed to a large number of high-energy complexes. The quantification of the heterogeneity of CO₂ adsorption sites, which is one of the main adsorption characteristics that can explain adsorption phenomena in detail, but is difficult to quantify, was also studied (Yang et al., 2021b). The distance between the C atom and the oxygen atom in the zeolite was found to be the heterogeneity indicator and it was influenced by the Na_{III} cations interactions.

6. Kinetic adsorption modelling

Kinetic adsorption and desorption analysis are crucial for process optimization. Understanding desorption kinetics is vital for the regeneration step, while adsorption kinetic is pivotal for sorbent development and process design engineering. Kinetic limitations are often the ones that hinder the launch of the process in practical use and need to be addressed properly.

The modelling of intrinsic kinetics of CO₂ adsorption on sorbents is often coupled with experimental work, which is used to verify the accuracy of theoretical simulation methods (Bos et al., 2019). Firstly, volumetric or gravimetric methods are implemented for the

measurement of the equilibrium adsorption capacity (q^*) of CO₂ and H₂O. The TGA uptake data are fitted by applying appropriate isotherm models for the determination of the adsorption parameters. Even though they provide a useful first evaluation of the sorbent, TGA experiments are conducted under a high flow rate, where the axial dispersion and heat effects are not as important as in DAC (Darunte et al., 2019). Therefore, q^* is next used as the input value for the kinetic LDF models, which simulate the CO₂ adsorption capacity against time. Several diverse CO₂ adsorption kinetic models have been explored for describing the TGA curves, namely the pseudo-first order model, pseudo-second order model, Avrami model, etc. (Kaur et al., 2020). The dynamic behaviour of the adsorption process is further described by the unsteady state fix bed models. They provide a more thorough insight into the CO₂ adsorption process in terms of production rate, energy requirement, and cost (Elfving, 2021).

6.1. CO₂ isotherm models

Adsorption equilibrium of CO₂ onto adsorbent material such as zeolites (Wilson and Tezel, 2020), amine-functionalized silica (Wurzbacher et al., 2011), polystyrene (Elfving et al., 2017a) or polypropylene resin (Wang et al., 2011) (Table S3) is usually estimated by using isotherm models (Chapter S4), where the adsorption capacity on solid-phase (q^*) is proportional to the adsorbate partial pressure in gas-phase. One of the most commonly used is classical Toth isotherm (Eq. S1, Fig. 4).

Several other models besides Toth's are employed to fit experimental data over a wide temperature range (Wang and LeVan, 2009). Elfving et al. (2017a) compared the Langmuir model, Freundlich (Eq. S5), Sips (Eq. S6), and a modified version of the classical Toth model (Eq. S7), which was proposed by Serna-Guerrero et al. (2010). The latter was found to best describe the experimental CO₂ capture capacity of polystyrene resin functionalized with a primary amine since one term described physisorption by the surface interaction and the second chemisorption by the amine groups.

However, only a narrow temperature range was studied (25–50 °C). To simulate winter conditions, they continued their research (Elfving et al., 2017b) at lower temperatures. The highest CO₂ adsorption capacities were achieved under cold temperatures by adding humidity in

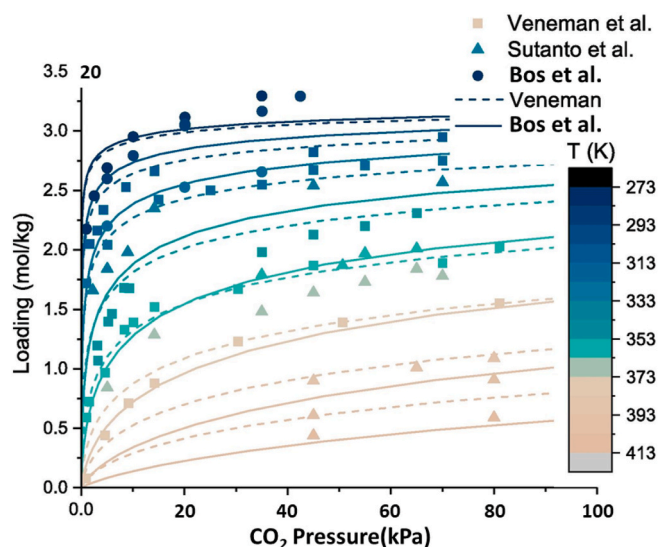


Fig. 4. Toth model fit (lines) to experimental adsorption capacity (markers) over a wide pressure and temperature range for Lewatit VP OC 1065 determined by Veneman et al. (2015) (squares), Sutanto et al. (2017) (triangles), and Bos et al. (2019) (circles). It indicates an indirect effect of the air temperature and CO₂ concentrations on the capture efficiency. Reproduced with permission (Bos et al., 2019). Copyright 2019 Elsevier.

the gas, up to $1.06 \text{ mmolCO}_2 \text{ g}^{-1}$. Nevertheless, any real-world design suffers from humid cold air. By comparing the performance of PSA, TSA, and TSVA, the first showed low equilibrium working capacity (WC) levels (Fig. 5), which is defined as the difference between CO_2 loading under adsorption and regeneration conditions. Quite the opposite, with TSA in dry and cold or warm and humid adsorption conditions, WC levels greater than $0.7 \text{ mmolCO}_2 \text{ g}^{-1}$ were achievable.

6.2. H_2O isotherm models

The co-adsorbed water can have both unfavourable or beneficial effects on CO_2 adsorption. It can increase the heat required for regeneration or, like in some cases of MOFs, can significantly enhance the degradation rate. On the contrary, the humidity present in amine-functionalized sorbents can increase CO_2 adsorption uptake capacity (Elfvig and Sainio, 2021). Toth isotherm has been used for H_2O adsorption modelling (Elfvig et al., 2017a, 2017b) but is inappropriate due to insufficient description of the multilayer adsorption behaviour in porous sorbents (Elfvig and Sainio, 2021). Instead, Guggenheim–Anderson–de Boer (GAB) isotherm model (Eq. S8, Fig. 6) is typically applied for equilibrium H_2O loading modelling as a function of relative humidity (RH) (Elfvig, 2021).

The vast majority of published models neglect the water effect on CO_2 isotherm or describe dry processes. Multicomponent competitive isotherms are not yet always available due to the novelty of the process, hence single component isotherms are used and an empirical description of the interaction of CO_2 and H_2O is done (Sabatino et al., 2021). Another study used the Langmuir-BET model for $\text{CO}_2/\text{H}_2\text{O}$ binary adsorption isotherms description (Z. Z. Wang et al., 2020). The monolayer CO_2 adsorption was described by the Langmuir model and multilayer H_2O adsorption was characterized by BET. However, the BET model is not temperature dependent and is inappropriate for amine-based sorbents. The adsorption capacity of CO_2 under humid conditions was also described by the Toth isotherm measured in dry conditions coupled with the empirical enhancing parameter (f_{RH}) (Deschamps et al., 2022; Wurzbacher et al., 2016). The CO_2 partial pressure and RH-dependent parameter are considered only when water is present. However, it was obtained by bilinear interpolation instead of co-adsorption isotherm modelling.

Detailed water and CO_2 co-adsorption isotherm models have been emerging lately. Stampi-Bombelli et al. (2020) modified the Toth model with two additional parameters, which reflect the enhancing water effect. Under humid conditions, the Toth isotherm parameters combined with water capacity increase the maximum CO_2 uptake and isotherm affinity, but in water absence, the model reduces to the single-component Toth isotherm. However, the parameters have no

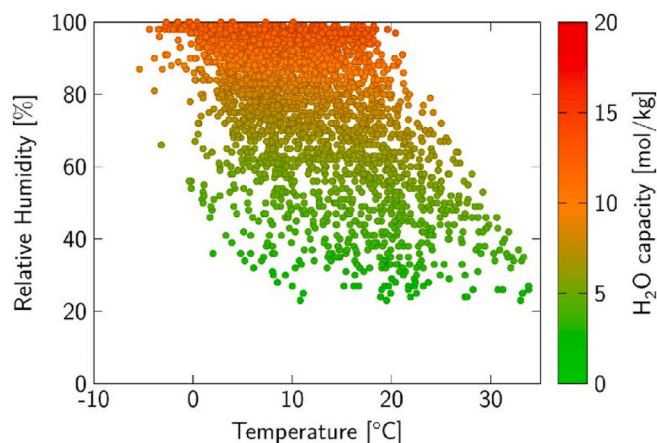


Fig. 6. The H_2O equilibrium capacity calculated from the GAB model for each combination of temperature and relative humidity for Lewatit VP OC 1065. The consideration of water presence is an important factor for efficient operation since it can have both hostile or beneficial effects on CO_2 adsorption. Reproduced with permission (Schellevis et al., 2021). Copyright 2021 Elsevier.

specific physical meaning and are always assumed to have a positive value. The model was compared to two novel mechanistic approaches to modelling co-adsorption equilibrium (Young et al., 2021) and was shown to overpredict the capacities at higher temperatures while requiring deeper vacuum pressure due to a higher affinity. The mechanistic co-adsorption model and the weighted average dual site Toth model showed an improved fit to experimental data compared to empirical models and were used for dynamic process model development (Young et al., 2021).

Further similar attempts of water presence consideration were done by exploiting the CO_2 and H_2O binding reaction mechanisms with the amine end of the PEI molecule to describe the reaction rate equations of CO_2 to carbamate and bicarbonate (Elfvig and Sainio, 2021; Jung and Lee, 2020). Langmuir-type kinetic models derived from the reaction mechanism showed that the moisture has not always a promoting effect and is depending on the temperature and mole fraction of CO_2 or H_2O in the gas phase. This was explained by competitive $\text{CO}_2/\text{H}_2\text{O}$ adsorption and reactions of carbamate and bicarbonate formation.

6.3. Linear driving force models

The rate of adsorption is controlled by several different transfer limitations, such as I) external mass transfer of CO_2 from the bulk to the sorbent surface, II) interparticle mass transfer from the sorbent surface

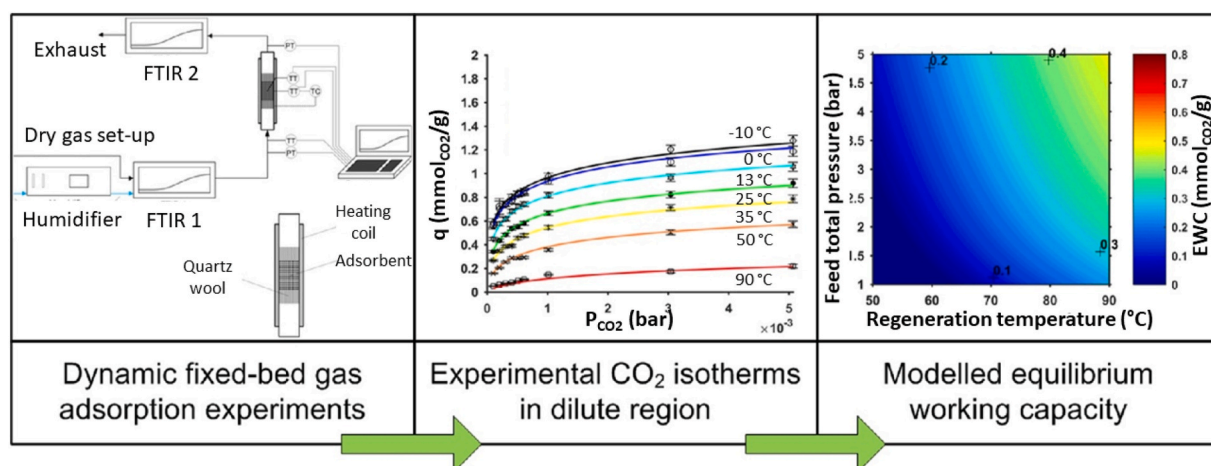


Fig. 5. Schematic representation of equilibrium working capacity calculation process. Reproduced with permission (Elfvig et al., 2017b). Copyright 2017 Elsevier.

to its interior, and III) physisorption or chemisorption. An appropriate mathematical description of all of the mentioned phenomena needs to be solved numerically by a set of complex partial differential equations, which can be computationally intensive. A proper alternative is simple, analytic, physically consistent, and frequently used linear driving force (LDF) model (Driessen et al., 2020).

Pseudo-first order kinetic model (Eq. (3)) is the most commonly applied due to its simplicity. Where two functional groups are needed for the capture of one CO₂ molecule, for example in dry amine-based sorbents, the pseudo-second order model (Eq. (4)) is more suitable due to a mechanistic point of view (Bos et al., 2019). Both were proposed by Lagergren (1989) and relate the adsorption rate to the number of vacant sites or square of available sites on the surface (Kaur et al., 2020).

$$\frac{\partial q}{\partial t} = k_{LDF,1}(q^* - q) \quad 3$$

$$\frac{\partial q}{\partial t} = k_{LDF,2}(q^* - q)^2 \quad 4$$

LDF models simulate the rate of CO₂ accumulation inside the particle and relate it to the difference between the average adsorbate concentration (q) at present conditions and the adsorbate concentration in equilibrium with the bulk concentration (q^*). The effective LDF mass transfer coefficient (k_{LDF}) integrates the mass transfer and reaction limitations. It is usually obtained by simple experimental data fitting to the model equations (Naidu and Mathews, 2021).

Three mathematical models, pseudo-first order, pseudo-second order, and Avrami kinetic (Eq. (5)) were compared for studying different adsorption characteristics of commercially available TEPA and PEI-loaded mesoporous silica SBA-15 composites (Miao et al., 2021). The Avrami kinetic model was found to best predict kinetic behaviour, even at low temperatures.

$$\frac{\partial q}{\partial t} = nk_{LDF,Avrami}t^{n-1}(q^* - q) \quad 5$$

The best sorbent material among the studied collection was 50% TEPA/SBA-15. Fast adsorption kinetics and high capture capacity were determined in a wide temperature range, at 25 °C being 2.30 mmolCO₂ g⁻¹. With amine loading increasing, the adsorption capacity also increased, but the diffusion barrier lowered the adsorption rate.

Al-Absi et al. (2022) also concluded that among the studied models the Avrami kinetic model best predicts the adsorption kinetics of CO₂ on the sorbent (Fig. 7). However, it overestimated the initial adsorption capacity, particularly at high RH. They also analysed mass transfer using the interparticle diffusion model (Eq. (6)), which illustrates the most basic approximation of pore diffusion kinetics. It was used to identify three mass transfer consecutive stages in the adsorption process (Fig. 8), namely external diffusion of CO₂ to the surface, interparticle diffusion,

and equilibrium establishment. The E_a increased by almost 40% and the enthalpy of adsorption almost doubled when changing the RH from 25% to 0%.

$$q = k_{id}t^{1/2} + C \quad 6$$

Pseudo-first order model approximated CO₂ diffusion into the particle and breakthrough experiments were also carried out for seven commercially available physisorbents to determine the optimal TVSA conditions (Wilson and Tezel, 2020). Low Si/Al ratio faujasite zeolite (APG-III) exhibited fast kinetics, high adsorption capacity (0.42 mmolCO₂ g⁻¹), high CO₂ selectivity but also high desorption energy requirement, and water removal demand.

Another LDF model definition was proposed by Glueckauf (Glueckauf, 1943; Glueckauf and Coates, 1947), who incorporated the CO₂ concentration in the form of partial pressure (P_{CO_2}) for a more theoretically consistent model (Eq. (7) and (8)). The comparison between Glueckauf's and Lagergren's model was presented by Rodrigues and Silva (2016). These equations were compared to the Toth rate equation (Eq. 9) by Bos et al. (2019). The latter was found to better describe the shape of the experimental curve since it describes both the temperature and pressure dependencies.

$$\frac{\partial q}{\partial t} = k_{LDF,1} P_{CO_2}(q^* - q) \quad 7$$

$$\frac{\partial q}{\partial t} = k_{LDF,2} P_{CO_2}(q^* - q)^2 \quad 8$$

$$\frac{\partial q}{\partial t} = k_{Toth} \left\{ P_{CO_2} \left[1 - \left(\frac{q}{q_s} \right)^{1/n} \right]^{\frac{1}{n}} - \frac{1}{b} \frac{q}{q_s} \right\} \quad 9$$

7. Unsteady state fixed bed dynamic process models

The adsorption and desorption behaviour on the adsorption bed is typically represented by a 1D or 2D dynamic model using finite element (finite difference or finite volume) methods (Chen et al., 2019), which consider both thermodynamics and kinetics. They are composed of a combination of partial differential and algebraic adsorbent bed equations, which include thermodynamics described by isotherms, mass and energy balances of gas and solid, and pressure drop along the column length described by the Ergun equation (Deschamps et al., 2022).

Mass transfer is governed by several different dispersive and mass transfer effects. The model evaluates the transfer rate in the film, macropore or micropore, the resistance-controlled diffusion and convection of the gas through the porous material, adsorption, desorption, and reaction kinetics (Darunte et al., 2019). Mass balance in the fixed bed can be defined as follows,

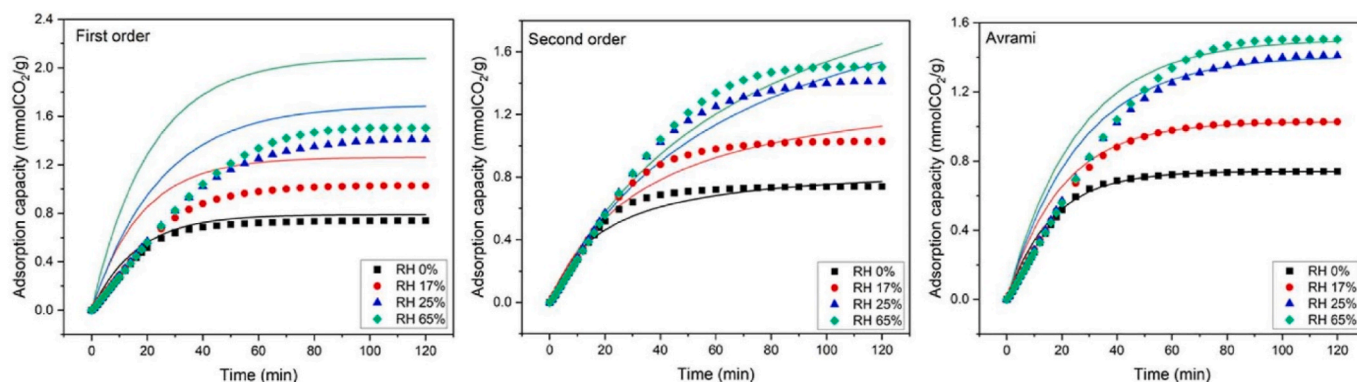


Fig. 7. The accuracy comparison between different LDF models applied. Experimental CO₂ uptake (markers) onto polyethylene amine tethered to mesoporous silica foam at different RH with the corresponding fit to pseudo-first, pseudo-second, and Avrami model (lines). These findings suggest that the Avrami kinetic model best predicts the adsorption kinetics. Reproduced with permission (Al-Absi et al., 2022). Copyright 2022 Elsevier.

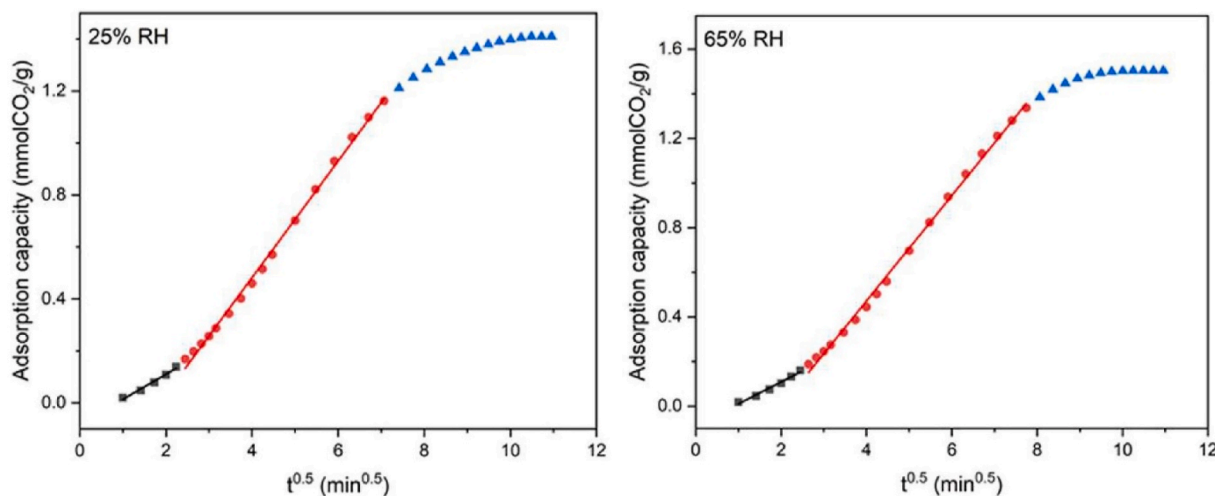


Fig. 8. Intra-particle diffusion model plot for CO₂ uptake at 25% RH and 65% RH, which identifies the three mass transfer consecutive stages in the adsorption process. Reproduced with permission (Al-Absi et al., 2022). Copyright 2022 Elsevier.

$$\frac{\partial C_b}{\partial t} + D_{ax} \frac{\partial^2 C_b}{\partial x^2} + \frac{\partial v_i C_b}{\partial x} + \frac{(1 - \varepsilon) \rho_p}{\varepsilon} \frac{\partial q_t}{\partial t} = 0 \quad (10)$$

where C_b is the CO₂ concentration in the bulk phase, D_{ax} is the axial dispersion coefficient, v_i is the interstitial velocity, ε is the bed porosity, ρ_p is the density of the particle, and q_t is the total adsorbed phase concentration (Knox et al., 2016).

The energy balances include the energy requirement of each DAC unit operation. It is a summation of the air blower specific energy consumption (Eq. (11)), the heat of adsorbent (Eq. (12)) and CO₂ (Eq. (13)), desorption heat of CO₂ (Eq. (14)), electrical energy required for the purge steam system, vacuum (Eq. (15)) and compression pump, etc. (Elfving, 2021). The major thermal energy consumer is usually column regeneration, while the major electrical energy consumers are the air blower, which needs to overcome the bed pressure drop due to the highly diluted air, and column evacuation (Deschamps et al., 2022; Stampi-Bombelli et al., 2020). Comparison of the modelled process properties reported in the literature is presented in Table 2.

$$E_{fan} = \int_0^t \Delta p \dot{V}_{tot} dt \quad (11)$$

$$E_{sen,a} = m_a c_{p,a} \Delta T \quad (12)$$

$$E_{sen,CO_2} = m_{CO_2} c_{p,CO_2} \Delta T \quad (13)$$

$$E_{des,CO_2} = \int_0^t (-\Delta H_{CO_2}) \dot{n}_{CO_2} dt \quad (14)$$

$$E_{vac} = -P_{out} \int_0^t \dot{V}_{tot} dt \left(\frac{P_1}{P_{out}} - \frac{P_2}{P_{out}} + \ln \left(\frac{P_2}{P_1} \right) \right) \quad (15)$$

7.1. Solid-supported amines

Simplified zero-dimensional models were developed for amine-based sorbents. The MSA desorption rate was defined by the Langmuir equation (Eq. 16) (Hou et al., 2017), or by modified equation by implying the partial CO₂ pressure as a function of saturation (Wang et al., 2013).

$$\frac{dq}{dt} = k_{ads}(1 - q)C - k_{des}q \quad (16)$$

More comprehensive and systematic analyses of the DAC process are conducted by 1D or 2D heat and mass transfer models. Studies show a huge impact of the kinetics on the performance, hence fast sorbent kinetic are desired (Zhu et al., 2021a).

Although most of the simulations conducted so far were performed at a laboratory scale, Deschamps et al. (2022) numerically evaluated the DAC process at a larger scale (50 tCO₂ y⁻¹), while conserving almost the same technology. The total electrical consumption was found to be very sensitive to the packed bed design ranging from 1000 kWh tCO₂⁻¹ to 3450 kWh tCO₂⁻¹ for lab- and industrial-scale, respectively.

7.1.1. Lewatit VP OC 1065

Lewatit VP OC 1065 is an ion-exchange resin, a polystyrene spherical sorbent with a benzylamine functional group, and one of the most explored amine sorbents due to its commercial availability. Moreover, it is believed to be comparable to Climeworks' first-generation adsorbent (Young et al., 2021).

Several works studied the influence of operational parameters on process performance. The higher gas flow was shown to not significantly contribute to higher energy duty, however, it improves productivity. Regeneration temperature was suggested to be as high as possible (Fig. 9) (Schellevis et al., 2021), but it should be understood as a selective tradeoff between high productivity and material stability (Young et al., 2021). The same beneficiary effect of high regeneration temperature was shown in the study of zeolite 13X (Zhang et al., 2022). Several studies emphasized the value of weather conditions consideration in the system design, most importantly air temperature and humidity. The more accurate representation of CO₂ and water co-adsorption by the novel mechanistic isotherm models led to an improved process model (Young et al., 2021).

Bos et al. (2019) explored the intrinsic kinetics of CO₂ adsorption by modelling convection, diffusion, and reaction rate. They numerically confirmed the assumption of the absence of mass and heat transfer limitations, which have been eliminated by the use of a bypass valve. A novel approach for modelling was used by Driessen et al. (2020) who proposed an effectiveness factor as a function of the Thiele modulus for a computationally un-intensive full model and two approximate methods development. The mathematical description of intraparticle mass transfer and intrinsic adsorption kinetics provided insight into the radial profiles of a spherical adsorbent particle. The solution illustrated the rate-determining steps, which were estimated by minimum and maximum Thiele modulus.

Whilst most of the modelling studies are based on the breakthrough experiments performed in fixed-bed reactors, Drechsler and Agar (2019) presented a novel moving belt adsorber concept (Fig. 10). The immobilized adsorbent bed on a moving supporting belt structure was moved through different process zones, while ensuring a maximum direct heat exchange, maximum possible CO₂ mole fraction in the gas phase, and

Table 2

Summarized modelled properties of DAC processes, allowing us to distinguish the best sorbents and process systems from among the many published by evaluating various criteria such as energy requirement, levelized cost, rate of CO₂ extraction, working capacity and desorption conditions.

Sorbent	Thermal (th) and electrical (ej) or total (tot) energy requirement	Levelized cost (\$ tCO ₂ ⁻¹)	Rate of CO ₂ extraction	Working capacity (mol kg ⁻¹)	Desorption conditions	Ref.
MOFs						
MOF-177	$1.3 \times 10^6 \text{ kWh}_{\text{th}} \text{ tCO}_2^{-1} + 1.35 \times 10^3 \text{ kWh}_e \text{ tCO}_2^{-1}$	39,400	4.5 kgCO ₂ h ⁻¹	3.9×10^{-4}	TSA 100 °C	Leonzio et al. (2022)
MOF-5	$4.94 \times 10^5 \text{ kWh}_{\text{th}} \text{ tCO}_2^{-1} + 1.52 \times 10^3 \text{ kWh}_e \text{ tCO}_2^{-1}$	16,300	4 kgCO ₂ h ⁻¹	8.4×10^{-4}	TSA 100 °C	Leonzio et al. (2022)
MIL-101	$1.07 \times 10^6 \text{ kWh}_{\text{th}} \text{ tCO}_2^{-1} + 1.54 \times 10^3 \text{ kWh}_e \text{ tCO}_2^{-1}$	66,600	4.5 kgCO ₂ h ⁻¹	3.5×10^{-4}	TSA 100 °C	Leonzio et al. (2022)
Mg-MOF-74	a	b	n/d	0.38	TSA 70 °C	Ji et al. (2022)
Zeolites						
Zeolite 13x	1.28 MJ _{tot} molCO ₂ ⁻¹	248	n/d	n/d	CSA 25 °C	Sinha et al. (2022)
Zeolite 13x	a	b	n/d	0.23	TSA 70 °C	Ji et al. (2022)
Zeolite 13x	8.73 MJ _{tot} molCO ₂ ⁻¹	n/d	n/d	n/d	TSA 100 °C	Zhang et al. (2022)
Zeolite 13x	2.2 MJ _{tot} molCO ₂ ⁻¹	n/d	n/d	n/d	TSA 95 °C	Santori et al. (2018)
Zeolite 5A	a	b	n/d	0.29	TSA 70 °C	Ji et al. (2022)
MOF supported amines						
MIL-101(Cr)-PEI-800	5.11 MJ _{tot} kgCO ₂ ⁻¹	75–140	n/d	n/d	TVSA saturated steam at 1 atm, 100 °C	Sinha et al. (2017)
MIL-101(Cr)-PEI-800	4.7–8.9 MJ _{tot} kgCO ₂ ⁻¹	n/d	6 kgCO ₂ m ⁻³ h ⁻¹	0.78	TVSA T _{max} = 120 °C, P _{min} = 10 kPa	Sabatino et al. (2021)
mmen-Mg2 (dobpdc)	3.6 MJ _{tot} kgCO ₂ ⁻¹	60–190	n/d	n/d	TVSA saturated steam at 1 atm, 100 °C	Sinha et al. (2017)
Silica supported amines						
SI-AEATPMS	$1.88 \times 10^3 \text{ kWh}_{\text{th}} \text{ tCO}_2^{-1} + 3.57 \times 10^2 \text{ kWh}_e \text{ tCO}_2^{-1}$	977	6.43 kgCO ₂ h ⁻¹	0.367	TSA 100 °C	Leonzio et al. (2022)
TRI-PE-MCM-41.	5962 MJ _{th} tCO ₂ ⁻¹ + 792 MJ _e tCO ₂ ⁻¹	~100	1.1 tCO ₂ unit ⁻¹ day ⁻¹	0.97	TSA 90 °C	Kulkarni and Sholl (2012)
Tri-PE-MCM-41	0.8–1.0 MJ _{th} kgCO ₂ ⁻¹ + 7.1–7.7 MJ _e kgCO ₂ ⁻¹	n/d	3.8–10.6 kgCO ₂ m ⁻³ h ⁻¹	0.638	TVSA T _{max} = 120 °C, P _{min} = 10 kPa	Sabatino et al. (2021)
Nanocellulose supported amines						
APDES-NFC-FD	$1.4 \times 10^3 \text{ kWh}_{\text{th}} \text{ tCO}_2^{-1} + 2.99 \times 10^2 \text{ kWh}_e \text{ tCO}_2^{-1}$	751	6.66 kgCO ₂ h ⁻¹	0.771	TSA 100 °C	Leonzio et al. (2022)
APDES-NFC	8.6–10.1 MJ _{th} kgCO ₂ ⁻¹ + 1.1–1.3 MJ _e kgCO ₂ ⁻¹	149–427	3.8–10.6 kgCO ₂ m ⁻³ h ⁻¹	0.314	TVSA T _{max} = 120 °C, P _{min} = 10 kPa	Sabatino et al. (2021)
APDES-NFC-FD	~ 0.3 MJ _{th} kgCO ₂ ⁻¹ + 35.5 MJ _e kgCO ₂ ⁻¹	n/d	2.45 × 10 ⁻⁵ kgCO ₂ h ⁻¹	n/d	TVSA 95 °C, 50 kPa	Stampi-Bombelli et al. (2020)
Lewatit VP OC 1065						
Lewatit VP OC 106	10.1–11.8 MJ _{th} kgCO ₂ ⁻¹ + 0.6–1.3 MJ _e kgCO ₂ ⁻¹	n/d	3.8–10.6 kgCO ₂ m ⁻³ h ⁻¹	0.68	TVSA T _{max} = 120 °C, P _{min} = 10 kPa	Sabatino et al. (2021)
Lewatit VP OC 1065	9.93 MJ _{th} kgCO ₂ ⁻¹ + 0.8 MJ _e kgCO ₂ ⁻¹	n/d	62.09 kg m ⁻³ day ⁻¹	0.91	TVSA 100 °C, 10–45 kPa	Young et al. (2021)
Lewatit VP OC 1065	22 MJ _{tot} kgCO ₂ ⁻¹	n/d	~0.2–0.35 kgCO ₂ day ⁻¹	0.6	TVSA 90 °C, 35 kPa	Schellevis et al. (2021)
Lewatit VP OC 1065	n/d	n/d	0.125 kgCO ₂ m ⁻¹ h ⁻¹	0.3	TSA 86 °C	Drechsler and Agar (2019)
Other not specifically defined solid-supported amines						
Solid supported amine	9.3 GJ _{th} tCO ₂ ⁻¹ + 100 kWh _e tCO ₂ ⁻¹	n/d	2.8 kgCO ₂ y ⁻¹	n/d	TVSA 110 °C, <30 kPa	Deschamps et al. (2022)
Solid supported amine	13.87 GJ _{th} tCO ₂ ⁻¹ + 3450 kWh _e tCO ₂ ⁻¹	n/d	50 tCO ₂ y ⁻¹	n/d	TVSA 110 °C, <30 kPa	Deschamps et al. (2022)
Solid supported amine	0.06 MJ _{th} molCO ₂ ⁻¹ + 0.238 MJ _e molCO ₂ ⁻¹	n/d	4.45 molCO ₂ kg ⁻¹ day ⁻¹	0.868	TVSA 90 °C, 40 kPa	Zhu et al. (2021a)
quaternary ammonium-based anion exchange resin	35.67 kJ _{tot} mol ⁻¹ c	34.68	n/d	n/d	MSA 45 °C, saturated water	Hou et al. (2017)
polystyrene resin-supported amine groups	n/d	n/d	n/d	0.5	PSA 0.1 kPa	Elfving et al. (2017b)
polystyrene resin-supported amine groups	n/d	n/d	n/d	0.74	TSA 50–60 °C	Elfving et al. (2017b)
polystyrene resin-supported amine groups	n/d	n/d	n/d	0.52	TVSA 90 °C, 0.05 kPa	Elfving et al. (2017b)
Solvent capture						
KOH, Ca(OH) ₂ Brentwood XF12560	8.81 GJ _{th} tCO ₂ ⁻¹ + 0 kWh _e tCO ₂ ⁻¹ or 5.25 GJ _{th} tCO ₂ ⁻¹ + 366 kWh _e tCO ₂ ⁻¹	94–232	1 MtCO ₂ y ⁻¹	n/d	Slaker; 300 °C, 100 kPa Calciner; 900 °C, 100 kPa compressed to 15 MPa	Keith et al. (2018)
KOH, Ca(OH) ₂ 250Y Sulzer packing	8.3–11.1 GJ _{tot} tCO ₂ ⁻¹	240–409	1 MtCO ₂ y ⁻¹	n/d	Slaker; 300 °C, 100 kPa Calciner; 900 °C, 100 kPa compressed to 15 MPa	An et al. (2022)

(continued on next page)

Table 2 (continued)

Sorbent	Thermal (t_{th}) and electrical (e_f) or total (t_{tot}) energy requirement	Levelized cost (\$ tCO ₂ ⁻¹)	Rate of CO ₂ extraction	Working capacity (mol kg ⁻¹)	Desorption conditions	Ref.
KOH, Ca(OH) ₂ M-250Y Sulzer packings	6.21–6.48 MJ _{tot} kgCO ₂ ⁻¹	419	0.18–0.45 kgCO ₂ m ⁻³ h ⁻¹	n/d	Slaker; 300 °C, 100 kPa Calcliner: 900 °C, 100 kPa	Sabatino et al. (2021)
NaOH Brentwood XF12560 packing	n/d	343 ^{d,e}	0.52 molCO ₂ m ⁻³ h ⁻¹	n/d	n/d	Holmes and Keith (2012)
MEA solution M-250Y Sulzer packings	20.1–49.32 MJ _{tot} kgCO ₂ ⁻¹	537	0.75–1.08 kgCO ₂ m ⁻³ h ⁻¹	n/d	Slaker; 300 °C, 100 kPa Calcliner: 900 °C, 100 kPa	Sabatino et al. (2021)
NaOH, Ca(OH) ₂ M-250Y Sulzer packings	8.1 GJ _{th} tCO ₂ ⁻¹ + 1.78 GJ _e tCO ₂ ⁻¹ or 210 MW _{th,reg} + 25 MW _{e,fan} + 38 MW _{e,reg} ^g	430,610 ^e	20 tCO ₂ m ⁻³ y ⁻¹ or 1 MtCO ₂ y ⁻¹	n/d	n/d	Socolow et al. (2011)
NaOH, Ca(OH) ₂ M-250Y Sulzer packings	210 MW _{th,reg} + 14 MW _{e,fan} + 38 MW _{e,reg} ^g	568 ^e	1 mCO ₂ y ⁻¹	n/d	n/d	Mazzotti et al. (2013)
NaOH, Ca(OH) ₂ M-500Y Sulzer packings	210 MW _{th,reg} + 13 MW _{e,fan} + 38 MW _{e,reg} ^f	556 ^e	1 mCO ₂ y ⁻¹	n/d	n/d	Mazzotti et al. (2013)
NaOH, Ca(OH) ₂ M-CC Sulzer packings	210 MW _{th,reg} + 12 MW _{e,fan} + 38 MW _{e,reg} ^f	518 ^e	1 mCO ₂ y ⁻¹	n/d	n/d	Mazzotti et al. (2013)

^a Concept of DAC integrated with HVAC, using the heat and energy of the condensation process for the desorption process. Energy consumption was not calculated, only exergy efficiency.

^b No extra cost since the energy is recovered from the HVAC system.

^c The study was based on the CO₂ capture as a sustainable gas fertilizer substitute in agriculture. The optimal conditions for providing CO₂ to the 3000 m³ big lettuce cultivation plant were 45 °C of desorption temperature and 3% of outlet CO₂ concentration. The plant did not reach high-purity CO₂ steam (≥95%) and hence the energy and cost requirements were not compared with the other methods.

^d Holmes and Keith (2012) only calculated the cost of air contactor cost (60 \$ tCO₂⁻¹) since it is the most unpredictable part of the regeneration process. The total cost calculation was adapted from APS' costing methodology.

^e Estimated avoided cost (the cost when net carbon is considered).

^f The total energy requirement is not reported. Instead, the heat required for regeneration and the electricity required to power the fans is shown.

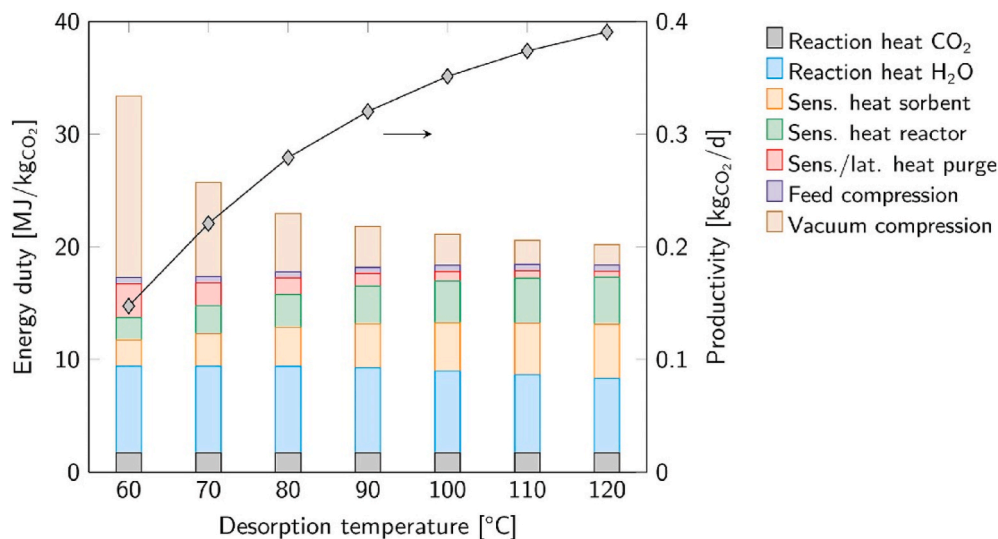


Fig. 9. Energy requirement for each DAC process unit as a function of desorption temperature. The results of this study indicate that the increasing desorption temperature lowers the energy requirement and increase the productivity. Reproduced with permission (Schellevis et al., 2021). Copyright 2021 Elsevier.

maximum contact time between the adsorbent and the stripping gas. More than 94% of the solid's heat needed for the reach of desorption temperature was recovered. The system operating in a TSA mode ensured the CO₂ mole fractions greater than 20% in the product flow of 0.125 kg m⁻¹ h⁻¹.

7.1.2. APDES-NFC-FD

Extended heat and mass transfer models of the DAC process based on packed bed TVSA or TSA technology for amine-functionalized nanofibrillated cellulose sorbent (APDES-NFC-FD) were developed greatly, especially by Wurzbacher's group. First, they examined the water and CO₂ coadsorption by varying the temperature and RH (Wurzbacher et al., 2012). The influence of the temperature on the adsorption profiles was found to be negligible. However, they confirmed the enhancing

effect of the RH on both CO₂ and H₂O uptake capacities. Moreover, they continued to study the process by developing an extended 2D heat and mass transfer model (Wurzbacher et al., 2016). The homogeneous gas phase composition across the sorbent bed was achieved due to the fast diffusion regardless of non-uniform heating. Under natural conditions (<10 kPa and >40% of relative humidity) more than 90% of the desorbed CO₂ could be recovered, while the purity levels surpassed 99%. Oxygen-induced degradation was prone to dry conditions and can be avoided by purging the air out by co-desorbed H₂O. Their further numerical modelling based on Climeworks AG's laboratory's experimental data examined the CO₂ and moisture adsorption effectiveness of the device used in the ventilation system (Kim et al., 2020). Several dynamic models developed by Deschamps et al. (2022), Leonzio et al. (2022) and Stampi-Bombelli et al. (2020) are based on their experimental results.

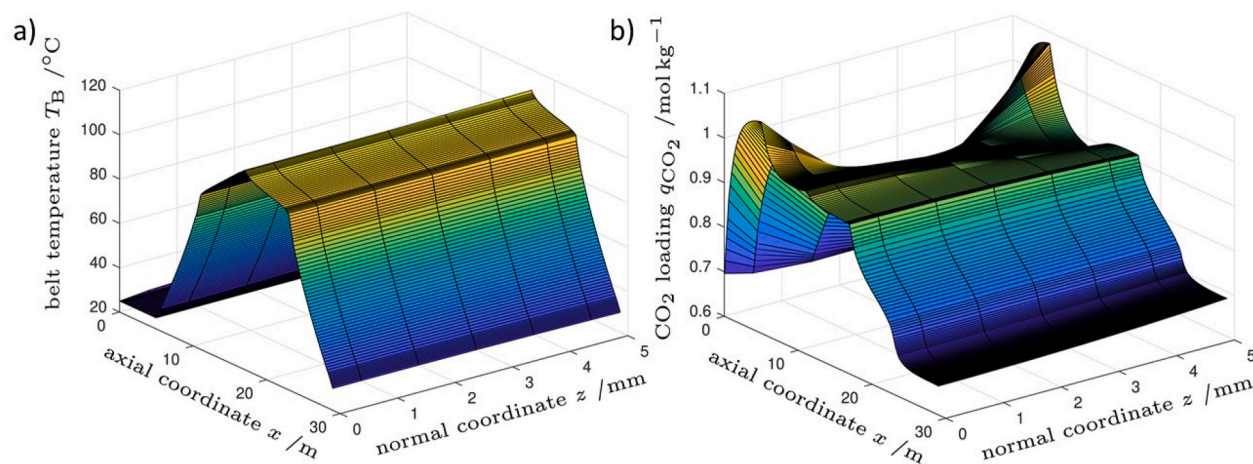


Fig. 10. a) Steady state temperature profile in the belt phase and b) steady state CO₂ loading profile on the sorbent material presenting a novel moving belt adsorber concept. Profiles are presented in the axial and normal direction coordinates. Reproduced with permission (Drechsler and Agar, 2019). Copyright 2019 Elsevier.

Moreover, the high productivity of the TVSA process was found to be limited due to the high porosity and low density of the APDES-NFC (Sabatino et al., 2021). The lower WC requires a higher regeneration temperature and lower vacuum pressure in comparison to other sorbents studied, resulting in energy requirements of 1.1–1.3 MJ_{el} kg⁻¹ and 8.6–10.1 MJ_{th} kg⁻¹. Stampi-Bombelli et al. (2020), who compared two TVSA cycle designs, steam assisted-TVSA, and regeneration via external heating, concluded that high evacuation pressures and low steam purge

rates were needed for energy reduction but yielded low CO₂ production rates. Steam purge accelerated desorption kinetics and hence contributed to higher CO₂ production rates at milder pressures, minimally reduced the electrical energy requirement but significantly increased the thermal energy consumption (Stampi-Bombelli et al., 2020). The higher amine content of the APDES-NFC-FD sorbent compared to SI-AEATPMS resulted in higher adsorption/desorption times, while the better performance was attributed to a lower mass transfer zone (Leonzio et al.,

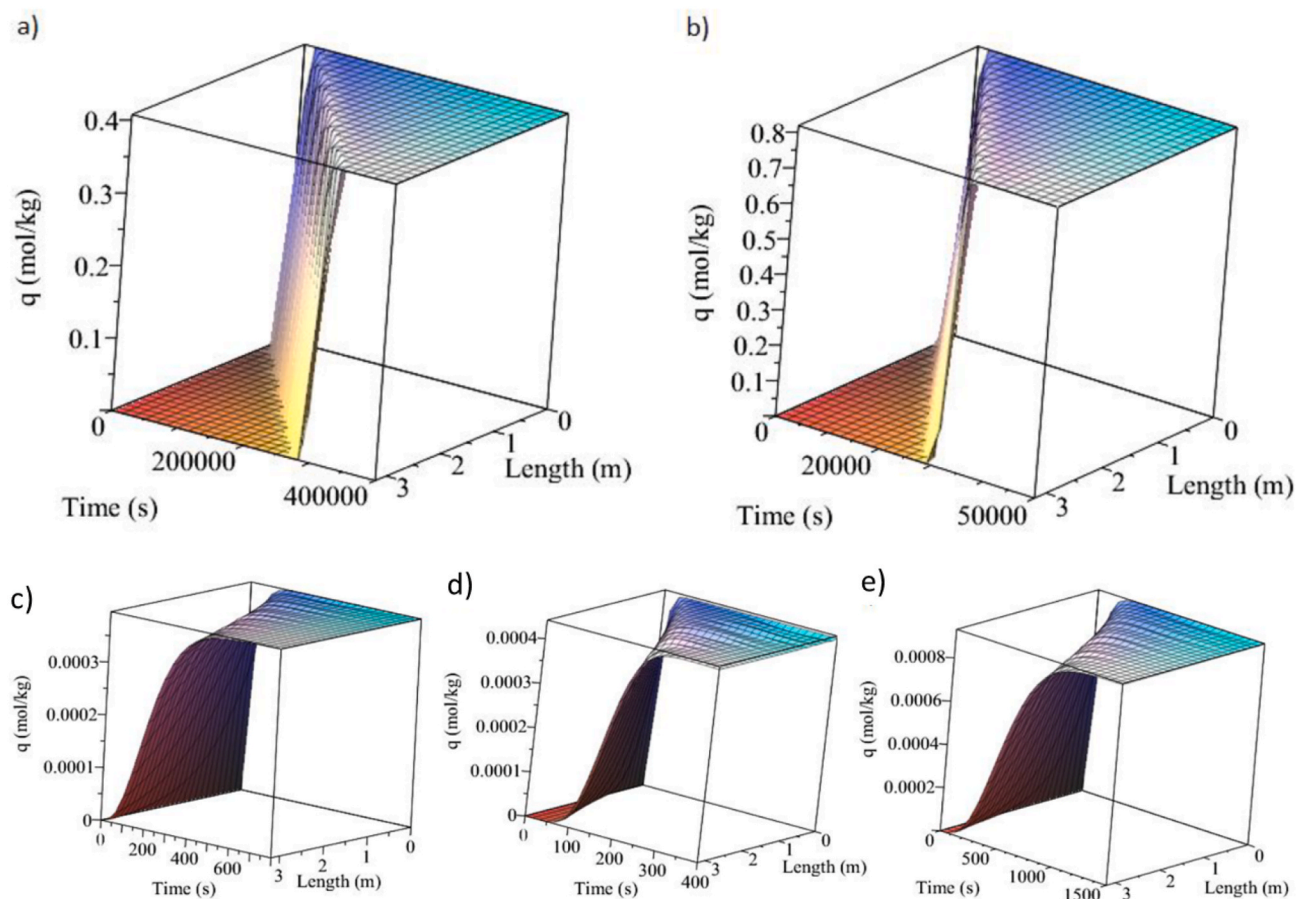


Fig. 11. CO₂ loading on chemisorbents a) SI-AEATPMS, b) APDES-NFC-FD and physisorbents c) MIL-101, d) MOF-177, and d) MOF-5 as a function of time and packed-bed length. The findings imply that chemisorbents display lower energy requirement and cost compared to physisorbents. Reproduced with permission (Leonzio et al., 2022). Copyright 2022 MDPI.

2022).

7.2. Zeolites and metal-organic frameworks

The built mathematical model by Leonzio et al. (2022) compared the adsorption and desorption behaviour of two amine-functionalized chemisorbents (SI-AEATPMS and APDES-NFC-FD) and three physisorbents (MIL-101, MOF-5, and MOF-177). Higher equilibrium loading of the firsts ($10^{-1} \text{ molCO}_2 \text{ g}^{-1}$) resulted in higher WC compared to the latter ($10^{-4} \text{ mmolCO}_2 \text{ g}^{-1}$) (Fig. 11). Thus, physisorbents exhibited much higher overall energy consumption ($10^6 \text{ kWh tCO}_2^{-1}$) and cost compared to chemisorbents ($10^3 \text{ kWh tCO}_2^{-1}$) (Leonzio et al., 2022). The amino-modified MOFs (MIL-101(Cr)-PEI-800) however exhibit performance comparable to the other reported amino-functionalized sorbents (Sabatino et al., 2021).

Another thermodynamic analysis of a 4-step TSA process compared three different physisorbent materials, namely zeolite 5A, zeolite 13X, and Mg MOF-74 (Ji et al., 2022). The DAC technology uses HVAC (heating, ventilation, and air conditioning) systems in the buildings (Fig. 12) as a thermal energy supplier, hence lower energy consumption and improvement in economics were expected. Modelling was applied for balance determination between adsorbent and three different refrigerants in HVAC. According to real WC (up to $0.38 \text{ mmolCO}_2 \text{ g}^{-1}$ at 70°C of desorption temperature) and coefficient of performance, integration of Mg-MOF-74 sorbent and R134a refrigerant exhibit the best performance for large CO_2 amounts. Taking both exergy efficiency (82%) and COP at 35°C into consideration, zeolite 13X and R134a exhibit superior efficiency in terms of energy requirement. Another gas capture system integration with the ventilation system was conducted by Sinha et al. (2022). They regulated CO_2 , O_2 , and humidity levels for energy reduction of air conditioning. The CO_2 levels were controlled by adsorption beds with zeolite 13X monoliths, while the humidity was controlled by silica gel. The proposed system resulted in 55% less energy consumption compared to conventional HVAC systems.

A five-step cyclic TVSA process (Fig. 13) using MOF adsorbent films (MIL-101(Cr)-PEI-800 and mmen-Mg2 (dobpdc)) on a monolithic substrate was modelled. Sinha et al. (2017) proposed energy requirement optimization by growing thicker adsorbent films and thinner monolithic walls or adsorbent use with higher equilibrium capacities. Thin walls decrease the structural stability and capture yields; however, thick films reduce their adherence stability to the wall. By using a wall thickness of $50 \mu\text{m}$ and a film thickness of $60 \mu\text{m}$, the minimum energy requirement for MIL-101(Cr)-PEI-800 and mmen-Mg2 (dobpdc) was $0.145 \text{ MJ molCO}_2^{-1}$ and $0.113 \text{ MJ molCO}_2^{-1}$, respectively. Furthermore, Darunte

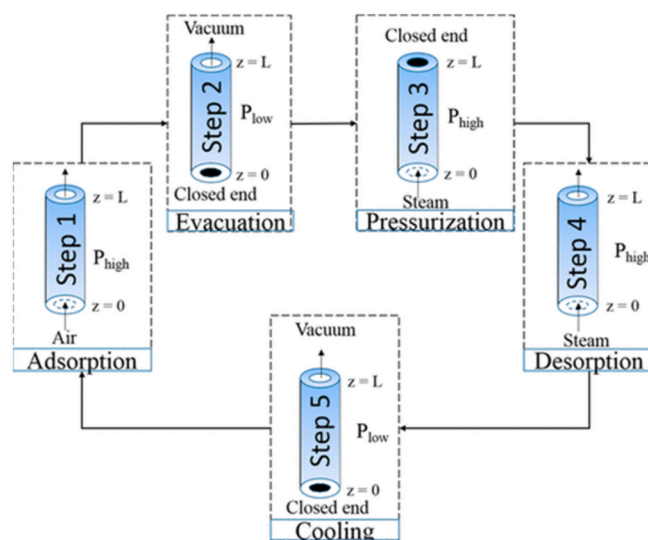


Fig. 13. The schematic representation of a five-step cyclic TVSA process. The study focused on the energy reduction and reached lower minimum energy requirement compared to the energy associated with the heat of combustion that produced the CO_2 . Reproduced with permission (Sinha et al., 2017). Copyright 2017 American Chemical Society.

et al. (2019) showed that the mass transfer was not much affected by the film and macropore resistances, but the limitations were hidden inside the crystal.

Moreover, a technology of a series of batch adsorption beds incorporating zeolite 13X and using solar thermal energy was modelled. Zhang et al. (2022) used the carbon pump theory to study energy consumption in thermodynamic analysis. After 120 cycles at 100°C of regeneration temperature, which required $8.73 \text{ MJ molCO}_2^{-1}$, a purity of 91% was reached. Santori et al. (2018) reached a high CO_2 purity ($>95\%$) and compared the zeolite 13X to another advanced material, zeolite NaETS-4. The latter reached higher purities at lower energy consumption, however, the technology required to filter large gas amounts resulting in high vacuum pump electricity consumption.

8. Lime-based sorbents

Even though the bulk of the modelling work so far has been done with amine sorbents, this state-of-the-art method is toxic, energy-

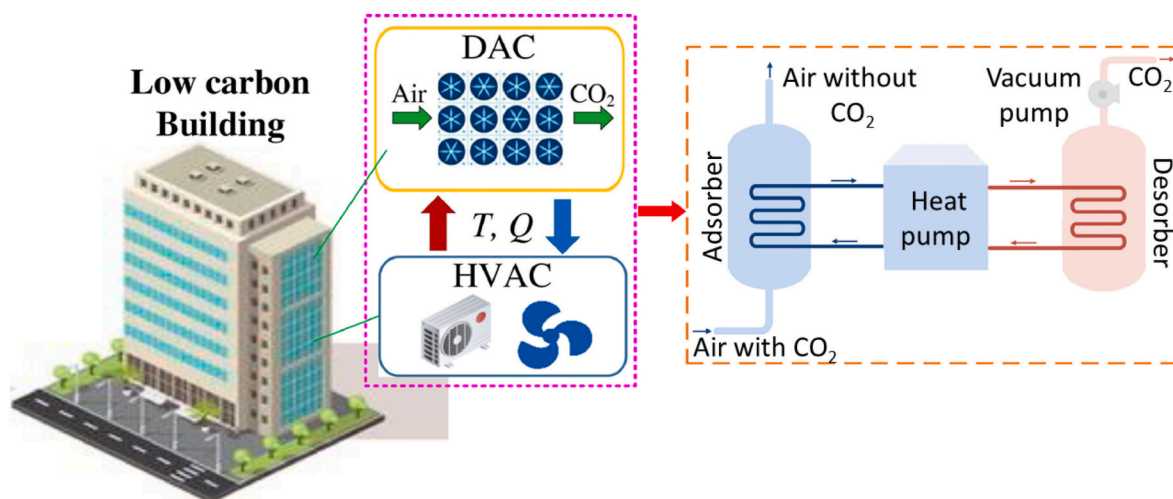


Fig. 12. Schematic diagram of DAC integrated with HVAC. This study provides support for the argument that using HVAC as thermal energy supplier reduces the overall energy consumption. Reproduced with permission (Ji et al., 2022). Copyright 2022 KeAi.

intensive, sensitive to impurities, and prone to degradation after periodic regeneration (Inkeri and Tynjälä, 2020). Lime-based sorbents, which store CO₂ in a form of bicarbonate, are earth-abundant and safe to use (McQueen et al., 2022). However, they are also known for their rapid decay in activity due to the sintering process, which can be mitigated by reactivation using moist air (Zeman, 2008).

An unreacted core kinetic model was used for the mathematical description of a three-step thermochemical CO₂ capture cycle. It includes intrinsic chemical reaction described by empirical Avrami rate laws followed by intra-particle diffusion (Nikulshina et al., 2007). Nonetheless, the small lime particles used in the study overcame the internal mass transfer limit in the vast majority.

Shrinking core model can be also applied for carbonation kinetics modelling (Samari et al., 2019). The model is straightforward and one of the most rudimentary for non-catalytic gas-solid reactions, since it does not demand the solid's structural parameters. The initial chemically-controlled step on the surface of the particle and the CaCO₃ formation is followed by carbonation, which is controlled by diffusion through the carbonate layer. Prehydrated sorbents and 55% of RH yielded the greatest carbonation conversions. (Samari et al., 2019). A kinetic grain model for flue gas capture showed that the reaction-controlled carbonation stage is pressure-dependent, while the diffusion-controlled rate is pressure and temperature-independent (Butler et al., 2014). DAC could be ultimately coupled with electrolysis to eventually produce e-fuels (Timmons and Terwel, 2022). Tregambi et al. (2022) numerically investigated catalytic methanation of CO₂ captured from CaO based DAC and hydrogen obtained from water electrolysis. For the production of one tonne of CH₄ the overall calculated energy demand varied between 344 and 370 GJ, while simultaneously removing 100 tCO₂ y⁻¹.

By comparing the performance of natural limestone and pelletized limestone, the latter was found to have higher effective diffusivity due to its greater porosity. Changing the particle size did not have a large effect on the surface reaction constants (Samari et al., 2019). Nevertheless, the larger mobilized particles are more prone to attrition, as demonstrated by a fluidized-bed reactor model, which described particle size distribution and attrition rate (Xiao et al., 2014).

9. Models based on the reaction mechanism

After conducting an evaluation of the most recent advances in kinetic and equilibrium of CO₂ adsorption modelling, comprehensive analyses which are based on reaction mechanisms of CO₂ adsorption are rarely found. However, this kind of model leads to improved consideration of the humidity effect and better fits of CO₂ isotherms (Elfving and Sainio, 2021). The model developed by Jung and Lee (2020) is based on the carbamate and bicarbonate formation reaction mechanism of amine-functionalized adsorbent. However, it neglected the reaction stoichiometry, the reactions had separated maximum capacities, the developed co-adsorption isotherm model resembled the dual-site Langmuir isotherm, and it was studied for CO₂ from flue gas. The shortcomings of this model were eliminated by Elfving and Sainio (2021). The isotherm and dynamic fixed-bed CO₂ adsorption modelling from air simulated the 0.87 mmolCO₂ g⁻¹ of starting CO₂ adsorption capacity and approximately 0.7% per cycle capacity drop rate.

The mechanism of moisture-controlled sorption in anion exchange materials was presented by Kaneko and Lackner (2022). Two limitations were considered, the domination of chemical reaction kinetics on pore surfaces and interior transport kinetics. A linear combination of first and second-order kinetics can describe the first case while applying the static isotherm equation. The second limitation can be expressed by a non-linear diffusion equation while using effective diffusivity that integrates the bicarbonate and carbonate diffusion coefficient. Generalized effective diffusivity (D_M) was also introduced for combining both limitations contributions and mainly depends on the membrane thickness. Slow CO₂ sorption was explained by low ion diffusivities under low

humidity, slow chemical reaction kinetics, and significant difference between the concentration and activity of each chemical species.

10. Solvent-based direct air capture

The idea of using an aqueous basic sorbent as an intermediate, coupled to a calcium caustic recovery loop is kinetically driven. CO₂ is first sorbed to KOH or NaOH and then transferred to Ca(OH)₂ due to the higher mass transfer coefficient (K_L) of the first and easier regeneration process for the second. The main consideration when designing the contactor is balancing the preferably high rate of mass transfer to the adsorbent with the pressure drop through the reactor (Realff et al., 2021).

One of the first leading NaOH aqueous Ca-looping technology research was published by the American Physical Society (APS) (Socolow et al., 2011) in 2011 and was further investigated and optimized by Mazzotti et al. (2013). Holmes and Keith (2012) showed that the highest influence on the process effectiveness have the solubility of CO₂ at the gas-liquid interface and the chemical reaction kinetics of CO₂ with NaOH. Each kg of NaOH adsorbs 20 g of CO₂ before regeneration takes place. Assuming the NaOH flux estimation of $\sim 4.1 \times 10^{-9}$ mol cm⁻² s⁻¹, 210 m² m⁻³ of specific packing Brentwood XF12560 area, 2 M NaOH, and 1 m contactor depth, the CO₂ uptake can reach 0.52 molCO₂ m⁻³ min⁻¹ (McQueen et al., 2021).

The solvent-based approaches require strong bases for adequate separation. Besides NaOH, KOH sorbent coupled to a calcium caustic recovery was also studied due to its faster kinetics with CO₂. Keith et al. (2018) presented an elaborate engineering research and cost analysis for 1 MtCO₂ y⁻¹ DAC plant and modelling for each individual unit of the process was performed (Fig. 14). Pilot plant performance data provided by Carbon Engineering enabled the design of a commercial scale reference process. The transport of CO₂ in the contactor was shown to be governed by the reaction processes and diffusion resistances present in the ~ 50 μm film of the KOH solution. The K_L is limited by [OH⁻] and temperature and not vastly by humidity. Modelled energy and mass balances led to an 8.81 GJ natural gas requirement or 5.25 GJ of gas and 366 kWh of electricity requirement for the capture of one ton of CO₂. Although the papers (Holmes et al., 2013; Holmes and Keith, 2012; Keith et al., 2018) form the basis for further studies, they were investigated under relatively moderate climate conditions. An et al. (2022) evaluated the influence of the air temperature and RH on the system performance. The impact of the first was already proven to be greater compared to the latter due to the exponential relationship between temperature and chemical reaction rates (Pinsent et al., 1956). The highest capture rates were accomplished under hot and humid conditions.

Another attempt to bypass amine-based capture technology is the use of water as a solvent (Inkeri and Tynjälä, 2020). The poor CO₂ solubility and high flow rates required were studied in a water bubble column reactor by a dynamic 1D multiphase model. Specific energy consumption was reduced by optimizing the gas flow rate, while the capture efficiency was maximized by increasing the liquid flow rate (Zhang et al., 2022).

Solvent and sorbent DAC types were also compared for performance evaluation. Two models describing adsorption/desorption behaviour on a NaOH solvent (Holmes and Keith, 2012) and PEI-functionalized cellulose acetate/silica sorbent (Kalyanaraman et al., 2015) were combined by Realff et al. (2021). The transport limitations of the solvent and sorbent systems were compared by adopting a hypothetical laminate contactor. The key result was that the CO₂ mass transfer across the liquid film was slower than the solid film adsorption at the same conditions. Also, the smaller contactor length in the solid compared to the liquid system has a favourable impact on the pressure drop. Another solid-solvent comparison was done by Sabatino et al. (2021), who performed an extensive study on costs assessment and optimization for TVSA DAC technologies based on two solvents (KOH and aqueous MEA solution) and 4 amine sorbents (APDES-NFC, Tri-PE-MCM-41, MIL-101

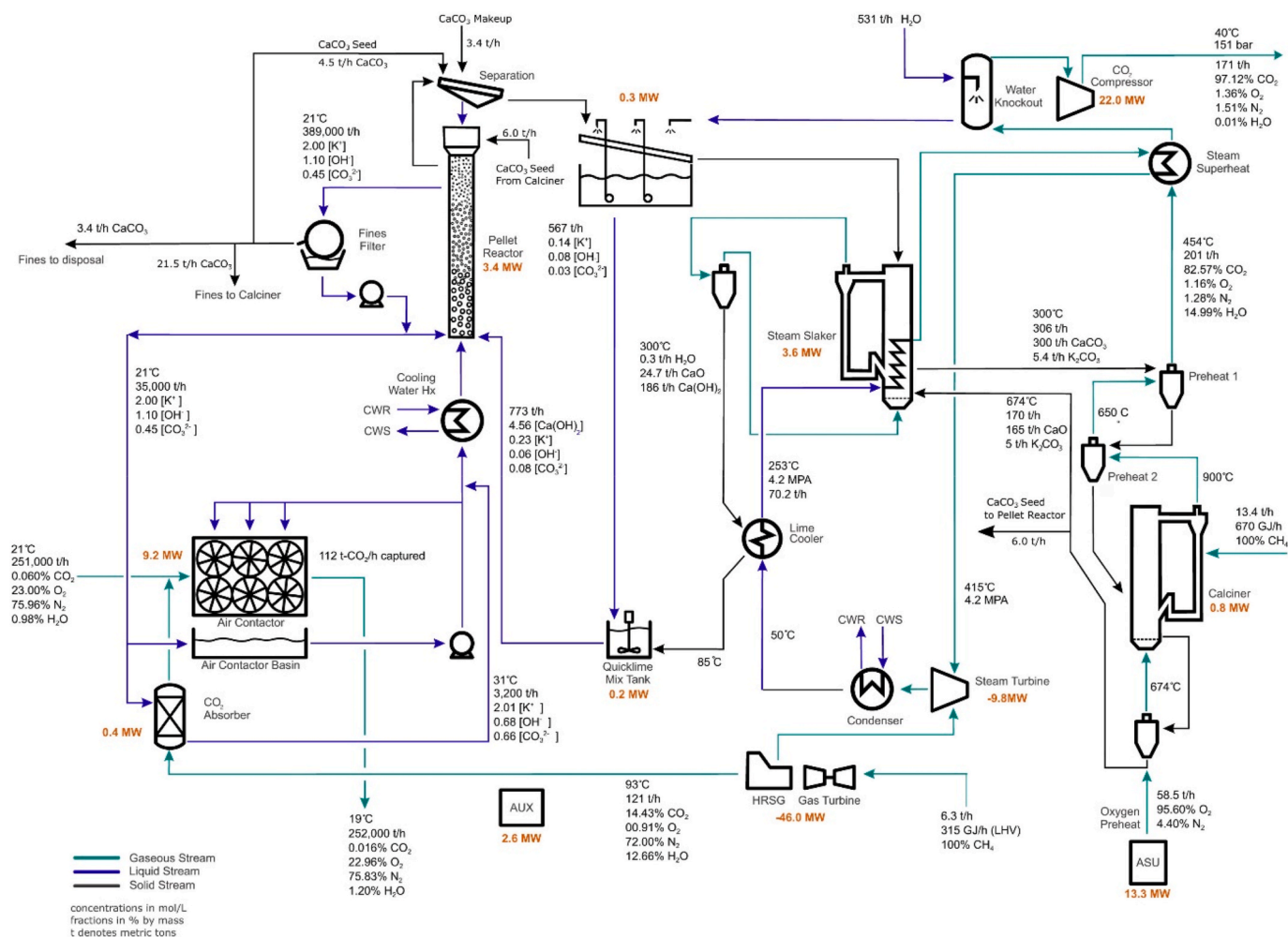


Fig. 14. A summary of mass and energy mass balance results of KOH sorbent coupled to a calcium caustic recovery presenting one of the most elaborated and important study in liquid DAC field. Reproduced with permission (Keith et al., 2018). Copyright 2018 Cell Press.

(Cr)-PEI-800, Lewatit VP OC 106). Solvent DAC processes exhibited much lower productivity ($0.18\text{--}1.08\text{ kgCO}_2\text{ m}^{-3}\text{ h}^{-1}$) in comparison to sorbent processes ($3.8\text{--}10.6\text{ kgCO}_2\text{ m}^{-3}\text{ h}^{-1}$). Despite the higher energy consumption by the amine solvent due to energy-intensive regeneration, all of the studied processes cost less than $200\text{ \$ tCO}_2^{-1}$. The purity of regenerated CO₂ was lower for alkali scrubbing (95%) in comparison to MEA (97%) due to MEA's outstanding selectivity. The remaining impurities consist of N₂, Ar, and O₂ and H₂O, N₂, and O₂ for alkali and amine scrubbing, respectively. The purity in the sorbent DAC is in the range of 94%–99%, where the main side product is water.

11. Computational fluid dynamic

While nano and mesoscale modelling support material development, macroscale modelling like computational fluid dynamic (CFD) is one of the best approaches to describe an idealized DAC system and to deploy the DAC at a large scale. Better selectivity, lower pressure drops and higher yields can be achieved by a good understanding of the interactions between the sorbent and reactive flow. Simulations enable the comparison between different geometries and types of structures. They give information on the fluid flow, pressure drops, suitable shape, structural simulations, heat transfer simulations, and sorbent loading. The main advantage of this numerical methodology based on the Navier-Stokes equation is the optimization of structures and acceleration of the development and design process (Huš et al., 2019).

CFD simulations for CO₂ capture from the post-combustion flue gas

were explored greatly, but CFD performance optimization still remains elusive. One of the few CDF studies simulated the CO₂ biofixation process by microalgae in the airlift reactor (Sadeghizadeh et al., 2018). A three-phase and 3D model based on the Euler-Euler approach comprised the hydrodynamic, unsteady state mass transfer and CO₂ fixation by biocatalyst and adsorption with chemical reaction. The maximum removal efficiency of CO₂ in two different input gas velocities of $7.458 \times 10^{-3}\text{ m s}^{-1}$ and $13.281 \times 10^{-3}\text{ m s}^{-1}$ were 84 and 67%, respectively. The simulation results deviated from the experimental data by less than 10%. Another biofixation study process in the microalgal attached membrane photobioreactor combined CFD with MD to investigate the synergy of light/fluid flow and membrane modification (Wang et al., 2022).

Moreover, using CFD simulations for aqueous KOH solvent, more than 30% pressure drop was observed by applying only a slight change to packing geometry in a commercial plant compared with the Brentwood XF12560 packing at the same external conditions (Keith et al., 2018). Hiltunen and Tynjälä (2016) also presented the CFD model for the DAC facility at the Neo-carbon Energy 6th Researcher's Seminar, however, no research papers are publicly available.

12. Conclusions

- Direct air capture is seen as a feasible option to reverse society's contribution to the increase in anthropogenic CO₂ emissions. However, even though considered as the state-of-the-art method, it is still

energy, resources, and cost prohibitive. In order to make the process economically and environmentally justified, multiscale modelling has been used as the leading tool for rapid sorbent screening and process design with minimized energy requirement.

- After conducting an evaluation of the most recent advances in DAC modelling research, several specific macroscale concepts like dynamic two-dimensional models are found. The lowest published DAC cost is 60 \$ tCO₂⁻¹. The DAC price range was set to 200–400 \$ tCO₂⁻¹, while the stated goal of most of the DAC companies is to reduce the cost below 100 \$ tCO₂⁻¹ due to extremely low CO₂ commercial prices. Among commercial pathways to DAC, Global Thermostat reported the lowest energy requirement. Only 150–260 kWh tCO₂⁻¹ and 1170–1410 kWh tCO₂⁻¹ of electrical and thermal energy are needed, respectively. MOF-supported amine sorbents exhibit low energy requirements, the lowest reported was 1000 kWh tCO₂⁻¹. The methods developed so far are generally not considered cost-competitive. The high capital and operating costs and limited demand for DAC due to the evolving societal view present a negative factor for the DAC technology progress.
- Several isotherm models are employed to fit experimental data for the calculation of the CO₂ adsorption equilibrium capacity onto adsorbent material. Most of the reported chemisorption sorbents have a capacity of CO₂ of over 1 mmol g⁻¹ under ambient conditions (at 400 ppm of CO₂), while physisorption sorbents typically exhibited much lower values. The vast majority of published models neglect the enhancing or diminishing water effect on CO₂ isotherm or describe dry processes. Multicomponent competitive isotherms lead to better representation of the adsorption breakthrough curves but are not yet always available due to the novelty of the DAC process.
- By imputing Monte Carlo simulation results into the saturation adsorption isotherm model, more accurate macroscopic adsorption properties can be predicted. However, MC simulations of the highly diluted gas mixtures require long runs for acceptable results.
- Nanoscale quantum mechanical modelling method, namely DFT, provided insight into the CO₂ capture mechanism for amino-functionalized sorbents. It also explained the thermodynamic water influence and the performance of MSA in PILs. The oxygen vacancy was identified as the reason for enhanced stability due to strong chemical interactions between MMOs and amines. Open metal ions in MOFs were discovered to be preferential adsorption sites.
- This review attempts to address knowledge gaps in nano, meso, and macroscale modelling, since several modelling techniques, like CFD performance optimization, fundamental for the improved unit outcome, still remains elusive.
- Several studies are focused on equilibrium CO₂ adsorption and adsorption kinetic models, but only a few under ultradilute and humid conditions, which are relevant for DAC. The bulk of the work so far has been done with CO₂ capture and its potential conversion. Whereas other gasses, such as NO_x and SO_x, are potential emerging resources especially close to point exhaust sources, near agriculture, cities, and heating plants. Greater challenges are posed by coupling the CO₂ capture with the sequestration, reactors, and neutralization of harmful environmental pollutants, monoxide, NO_x, and SO_x or ultimately with electrolysis for e-fuel production.

Declaration of competing interest

The authors declare that they have no known competing financial interests or personal relationships that could have appeared to influence the work reported in this paper.

Data availability

No data was used for the research described in the article.

Acknowledgements

This research was funded by the Slovenian Research Agency (ARRS) through Programme P2–0152 and the research projects J1-3028, J2-1723, and J7-1816.

Appendix A. Supplementary data

Supplementary data to this article can be found online at <https://doi.org/10.1016/j.jclepro.2023.137185>.

References

- Afonso, R., Sardo, M., Mafra, L., Gomes, J.R.B., 2019. Unravelling the structure of chemisorbed CO₂ species in mesoporous aminosilicas: a critical survey. *Environ. Sci. Technol.* 53, 2758–2767. <https://doi.org/10.1021/acs.est.8b05978>.
- Al-Absi, A.A., Mohamedali, M., Domin, A., Benneker, A.M., Mahinpey, N., 2022. Development of in situ polymerized amines into mesoporous silica for direct air CO₂ capture. *Chem. Eng. J.* 447, 137465 <https://doi.org/10.1016/j.cej.2022.137465>.
- An, K., Farooqui, A., McCoy, S.T., 2022. The impact of climate on solvent-based direct air capture systems. *Appl. Energy* 325. <https://doi.org/10.1016/j.apenergy.2022.119895>.
- Anila, S., Suresh, C.H., 2021. Guanidine as a strong CO₂ adsorbent: a DFT study on cooperative CO₂ adsorption. *Phys. Chem. Chem. Phys.* 23, 13662–13671. <https://doi.org/10.1039/d1cp00754h>.
- Arstad, B., Blom, R., Swang, O., 2007. CO₂ absorption in aqueous solutions of alkanolamines: mechanistic insight from quantum chemical calculations. *J. Phys. Chem. A* 111, 1222–1228. <https://doi.org/10.1021/jp065301v>.
- Bernini, M.C., García Blanco, A.A., Villarroel-Rocha, J., Fairen-Jimenez, D., Sapag, K., Ramirez-Pastor, A.J., Narda, G.E., 2015. Tuning the target composition of amine-grafted CPO-27-Mg for capture of CO₂ under post-combustion and air filtering conditions: a combined experimental and computational study. *Dalton Trans.* 44, 18970–18982. <https://doi.org/10.1039/c5dt03137k>.
- Bien, C.E., Liu, Q., Wade, C.R., 2020. Assessing the role of metal identity on CO₂ adsorption in MOFs containing M-OH functional groups. *Chem. Mater.* 32, 489–497. <https://doi.org/10.1021/acs.chemmater.9b04228>.
- Bos, M.J., Kreuger, T., Kersten, S.R.A., Brilman, D.W.F., 2019. Study on transport phenomena and intrinsic kinetics for CO₂ adsorption in solid amine sorbent. *Chem. Eng. J.* 377, 1–13. <https://doi.org/10.1016/j.cej.2018.11.072>.
- Bos, M.J., Kersten, S.R.A., Brilman, D.W.F., 2020. Wind power to methanol: renewable methanol production using electricity, electrolysis of water and CO₂ air capture. *Appl. Energy* 264. <https://doi.org/10.1016/j.apenergy.2020.114672>.
- Breyer, C., Fasihi, M., Bajamundi, C., Creutzig, F., 2019. Direct air capture of CO₂: a key technology for ambitious climate change mitigation. *Joule* 3, 2053–2057. <https://doi.org/10.1016/j.joule.2019.08.010>.
- Buijs, W., 2019a. Direct air capture of CO₂ with an amine resin: a molecular modeling study of the oxidative deactivation mechanism with O₂. *Ind. Eng. Chem. Res.* 58, 17760–17767. <https://doi.org/10.1021/acs.iecr.9b03823>.
- Buijs, W., 2019b. Direct air capture of CO₂ with an amine resin: a molecular modeling study of the deactivation mechanism by CO₂. *Ind. Eng. Chem. Res.* 58, 14705–14708. <https://doi.org/10.1021/acs.iecr.9b02637>.
- Buijs, W., De Flart, S., 2017. Direct air capture of CO₂ with an amine resin: a molecular modeling study of the CO₂ capturing process. *Ind. Eng. Chem. Res.* 56, 12297–12304. <https://doi.org/10.1021/acs.iecr.7b02613>.
- Butler, J.W., Jim Lim, C., Grace, J.R., 2014. Kinetics of CO₂ absorption by CaO through pressure swing cycling. *Fuel* 127, 78–87. <https://doi.org/10.1016/j.fuel.2013.09.058>.
- Chanajaree, R., Chokbunpiam, T., Kärger, J., Hannongbua, S., Fritzsche, S., 2019. Investigating adsorption- and diffusion selectivity of CO₂ and CH₄ from air on zeolitic imidazolate Framework-78 using molecular simulations. *Microporous Mesoporous Mater.* 274, 266–276. <https://doi.org/10.1016/j.micromeso.2018.07.023>.
- Chen, Q., Rosner, F., Rao, A., Samuelsen, S., Jayaraman, A., Alptekin, G., 2019. Simulation of elevated temperature solid sorbent CO₂ capture for pre-combustion applications using computational fluid dynamics. *Appl. Energy* 237, 314–325. <https://doi.org/10.1016/j.apenergy.2019.01.042>.
- Coskuner, Y.B., 2018. A Grand Canonical Monte Carlo Simulation Model for Phase Behavior of Confined Hydrocarbons 57.
- Darunte, L.A., Sen, T., Bhawanani, C., Walton, K.S., Sholl, D.S., Realf, M.J., Jones, C.W., 2019. Moving beyond adsorption capacity in design of adsorbents for CO₂ capture from ultradilute feeds: kinetics of CO₂ adsorption in materials with stepped isotherms. *Ind. Eng. Chem. Res.* 58, 366–377. <https://doi.org/10.1021/acs.iecr.8b05042>.
- Deng, X., Yang, W., Li, S., Liang, H., Shi, Z., Qiao, Z., 2020. Large-scale screening and machine learning to predict the computation-ready, experimental metal-organic frameworks for CO₂ capture from air. *Appl. Sci.* 10 <https://doi.org/10.3390/app10020569>.
- Deng, Y., Li, J., Miao, Y., Izkowitz, D., 2021. A comparative review of performance of nanomaterials for Direct Air Capture. *Energy Rep.* 7, 3506–3516. <https://doi.org/10.1016/j.egy.2021.06.002>.

- Deschamps, T., Kanniche, M., Grandjean, L., Authier, O., 2022. Modeling of vacuum temperature swing adsorption for direct air capture using aspen adsorption. *Cleanroom Technol.* 4, 258–275. <https://doi.org/10.3390/cleantechnol4020015>.
- Dietzel, P.D.C., Johnsen, R.E., Fjellvåg, H., Bordiga, S., Groppo, S., Blom, R., 2008. Adsorption properties and structure of CO₂ adsorbed on open coordination sites of metal-organic framework Ni₂(dhtp) from gas adsorption, IR spectroscopy and X-ray diffraction. *Chem. Commun.* 2, 5125–5127. <https://doi.org/10.1039/b810574j>.
- Ding, M., Flaig, R.W., Jiang, H.L., Yaghi, O.M., 2019. Carbon Capture and Conversion Using Metal-Organic Frameworks and MOF-Based Materials. *Chemical Society Reviews*. <https://doi.org/10.1039/c8cs00829a>.
- Drechsler, C., Agar, D.W., 2019. Simulation and optimization of a novel moving belt adsorber concept for the direct air capture of carbon dioxide. *Comput. Chem. Eng.* 126, 520–534. <https://doi.org/10.1016/j.compchemeng.2019.04.023>.
- Driessen, R.T., Kersten, S.R.A., Brilman, D.W.F., 2020. A Thiele modulus approach for nonequilibrium adsorption processes and its application to CO₂ capture. *Ind. Eng. Chem. Res.* 59, 6874–6885. <https://doi.org/10.1021/acs.iecr.9b05503>.
- Elfving, J., 2021. Direct Capture of CO₂ from Air Using Amine-Functionalized Resin - Effect of Humidity in Modelling and Evaluation of Process Concepts.
- Elfving, J., Sainio, T., 2021. Kinetic approach to modelling CO₂ adsorption from humid air using amine-functionalized resin: equilibrium isotherms and column dynamics. *Chem. Eng. Sci.* 246, 116885 <https://doi.org/10.1016/j.ces.2021.116885>.
- Elfving, J., Bajamundi, C., Kauppinen, J., 2017a. Characterization and performance of direct air capture sorbent. *Energy Proc.* 114, 6087–6101. <https://doi.org/10.1016/j.egypro.2017.03.1746>.
- Elfving, J., Bajamundi, C., Kauppinen, J., Sainio, T., 2017b. Modelling of equilibrium working capacity of PSA, TSA and TVSA processes for CO₂ adsorption under direct air capture conditions. *J. CO₂ Util.* 22, 270–277. <https://doi.org/10.1016/j.jcou.2017.10.010>.
- Erans, M., Sanz-Pérez, E.S., Hanak, D.P., Clulow, Z., Reiner, D.M., Mutch, G.A., 2022. Direct air capture: process technology, techno-economic and socio-political challenges. *Energy Environ. Sci.* 15, 1360–1405. <https://doi.org/10.1039/d1ee03523a>.
- Fasihi, M., Efimova, O., Breyer, C., 2019. Techno-economic assessment of CO₂ direct air capture plants. *J. Clean. Prod.* 224, 957–980. <https://doi.org/10.1016/j.jclepro.2019.03.086>.
- Galimova, T., Ram, M., Bogdanov, D., Fasihi, M., Khalili, S., Gulagi, A., Karjunen, H., Mensah, T.N.O., Breyer, C., 2022. Global demand analysis for carbon dioxide as raw material from key industrial sources and direct air capture to produce renewable electricity-based fuels and chemicals. *J. Clean. Prod.* 373 <https://doi.org/10.1016/j.jclepro.2022.133920>.
- Glueckauf, E., 1943. Theory of chromatography, part 10- Formulae for diffusion into spheres and their application to chromatography. *Nature* 152, 220. <https://doi.org/10.1016/b978-0-08-057178-2.50005-4>.
- Glueckauf, E., Coates, J.I.I., 1947. The influence of incomplete equilibrium on the front boundary of chromatogram and on the effectiveness of SepuTation. *Theory of Chromatography* 1315–1321.
- Guo, Y., Gou, X., Xu, Z., Skare, M., 2022. Carbon pricing mechanism for the energy industry: a bibliometric study of optimal pricing policies. *Acta Montan. Slovaca* 27, 49–69. <https://doi.org/10.46544/AMS.v27i1.05>.
- Hiltunen, H., Tynjälä, T., 2016. Modelling of Direct Air Capture of CO₂ with Fluent. *Neo-Carbon Energy 6th Researcher's Seminar*.
- Holmes, G., Keith, D.W., 2012. An air-liquid contactor for large-scale capture of CO₂ from air. *Phil. Trans. Math. Phys. Eng. Sci.* 370, 4380–4403. <https://doi.org/10.1098/rsta.2012.0137>.
- Holmes, G., Nold, K., Walsh, T., Heidel, K., Henderson, M.A., Ritchie, J., Klavins, P., Singh, A., Keith, D.W., 2013. Outdoor prototype results for direct atmospheric capture of carbon dioxide. In: *Energy Procedia*. Elsevier Ltd, pp. 6079–6095. <https://doi.org/10.1016/j.egypro.2013.06.537>.
- Hou, C., Wu, Y., Jiao, Y., Huang, J., Wang, T., Fang, M., Zhou, H., 2017. Integrated direct air capture and CO₂ utilization of gas fertilizer based on moisture swing adsorption. *J. Zhejiang Univ. - Sci.* 18, 819–830. <https://doi.org/10.1631/jzus.A1700351>.
- Huš, M., Grilc, M., Pavličič, A., Likozar, B., Hellman, A., 2019. Multiscale modelling from quantum level to reactor scale: an example of ethylene epoxidation on silver catalysts. *Catal. Today* 338, 128–140. <https://doi.org/10.1016/j.cattod.2019.05.022>.
- Inkeri, E., Tynjälä, T., 2020. Modeling of CO₂ capture with water bubble column reactor. *Energies* 13. <https://doi.org/10.3390/en13215793>.
- International Energy Agency, I., 2022. *Direct Air Capture: A Key Technology for Net Zero*.
- Ji, Y., Yong, J.Y., Liu, W., Zhang, X.J., Jiang, L., 2022. Thermodynamic Analysis on Direct Air Capture for Building Air Condition System: Balance between Adsorbent and Refrigerant. *Energy and Built Environment*. <https://doi.org/10.1016/j.enbenv.2022.02.009>.
- Jung, W., Lee, K.S., 2020. Isotherm and kinetics modeling of simultaneous CO₂ and H₂O adsorption on an amine-functionalized solid sorbent. *J. Nat. Gas Sci. Eng.* 84, 103489 <https://doi.org/10.1016/j.jngse.2020.103489>.
- Kalyanaraman, J., Fan, Y., Lively, R.P., Koros, W.J., Jones, C.W., Realf, M.J., Kawajiri, Y., 2015. Modeling and experimental validation of carbon dioxide sorption on hollow fibers loaded with silica-supported poly(ethylenimine). *Chem. Eng. J.* 259, 737–751. <https://doi.org/10.1016/j.cej.2014.08.023>.
- Kaneko, Y., Lackner, K.S., 2022. Kinetic model for moisture-controlled CO₂ sorption. *Phys. Chem. Chem. Phys.* 21061–21077. <https://doi.org/10.1039/d2cp02440c>.
- Kaur, B., Gupta, R.K., Bhunia, H., 2020. CO₂ capture on activated carbon from PET (polyethylene terephthalate) waste: kinetics and modeling studies. *Chem. Eng. Commun.* 207, 1031–1047. <https://doi.org/10.1080/00986445.2019.1635466>.
- Keith, D.W., Holmes, G., st Angelo, D., Heidel, K., 2018. A process for capturing CO₂ from the atmosphere. *Joule* 2, 1573–1594. <https://doi.org/10.1016/j.joule.2018.05.006>.
- Kim, M.K., Baldini, L., Leibundgut, H., Wurzbacher, J.A., 2020. Evaluation of the humidity performance of a carbon dioxide (CO₂) capture device as a novel ventilation strategy in buildings. *Appl. Energy* 259, 112869. <https://doi.org/10.1016/j.apenergy.2019.03.074>.
- Knox, J.C., Ebner, A.D., Levan, M.D., Coker, R.F., Ritter, J.A., 2016. Limitations of breakthrough curve analysis in fixed-bed adsorption. *Ind. Eng. Chem. Res.* 55, 4734–4748. <https://doi.org/10.1021/acs.iecr.6b00516>.
- Kong, X., Scott, E., Ding, W., Mason, J.A., 2012. 4410 ftp, *Understanding CO₂ Dynamics in Metal-Organic Frameworks with Open Metal Sites*. Pdf.
- Kulkarni, A.R., Sholl, D.S., 2012. Analysis of equilibrium-based TSA processes for direct capture of CO₂ from Air. *Ind. Eng. Chem. Res.* 51, 8631–8645. <https://doi.org/10.1021/ie300691c>.
- Lackner, K., Ziock, H., Grimes, P., 1999. In: *Carbon Dioxide Extraction from Air: Is it an Option?* 24th Annual Technical Conference on Coal Utilization & Fuel Systems 1–12.
- Lagergren, S.Y.D., 1899. About the theory of so-called adsorption of soluble substances. *K. - Sven. Vetenskapsakademiens Handl.* 24, 1–39.
- Lee, Y.Y., Edgehouse, K., Klemm, A., Mao, H., Pentzer, E., Gurkan, B., 2020. Capsules of reactive ionic liquids for selective capture of carbon dioxide at low concentrations. *ACS Appl. Mater. Interfaces* 12, 19184–19193. <https://doi.org/10.1021/acsami.0c01622>.
- Lee, J.W., Ahn, H., Kim, S., Kang, Y.T., 2023. Low-concentration CO₂ capture system with liquid-like adsorbent based on monoethanolamine for low energy consumption. *J. Clean. Prod.* 390, 136141 <https://doi.org/10.1016/j.jclepro.2023.136141>.
- Leonzio, G., Fennel, P.S., Shah, N., 2022. A comparative study of different sorbents in the context of direct air capture (DAC): evaluation of key performance indicators and comparisons. *Appl. Sci.* 12 <https://doi.org/10.3390/app12052618>.
- Li, K., Kress, J.D., Mebane, D.S., 2016. The mechanism of CO₂ adsorption under dry and humid conditions in mesoporous silica-supported amine sorbents. *J. Phys. Chem. C* 120, 23683–23691. <https://doi.org/10.1021/acs.jpcc.6b08808>.
- Maroušek, J., Gavurová, B., 2022. Recovering phosphorus from biogas fermentation residues indicates promising economic results. *Chemosphere* 291. <https://doi.org/10.1016/j.chemosphere.2021.133008>.
- Mazzotti, M., Baciocchi, R., Desmond, M.J., Socolow, R.H., 2013. Direct air capture of CO₂ with chemicals: optimization of a two-loop hydroxide carbonate system using a counter-current air-liquid contactor. *Clim. Change* 118, 119–135. <https://doi.org/10.1007/s10584-012-0679-y>.
- McQueen, N., Gomes, K.V., McCormick, C., Blumanthal, K., Pisciotta, M., Wilcox, J., 2021. A review of direct air capture (DAC): scaling up commercial technologies and innovating for the future. *Progress in Energy* 3, 032001. <https://doi.org/10.1088/2516-1083/abf1ce>.
- McQueen, N., Ghoussoub, M., Mills, J., Scholten, M., 2022. A scalable direct air capture process based on accelerated weathering of calcium hydroxide. *Heirloom Carbon Technologies* 1–9.
- Miao, Y., He, Z., Zhu, X., Izikowitz, D., Li, J., 2021. Operating temperatures affect direct air capture of CO₂ in polyamine-loaded mesoporous silica. *Chem. Eng. J.* 426, 131875 <https://doi.org/10.1016/j.cej.2021.131875>.
- Miller, D.C., Syamali, M., Mebane, D.S., Storlie, C., Bhattacharyya, D., Sahinidis, N.V., Agarwal, D., Tong, C., Zitney, S.E., Sarkar, A., Sun, X., Sundaresan, S., Ryan, E., Engel, D., Dale, C., 2014. Carbon capture simulation initiative: a case study in multiscale modeling and new challenges. *Annu. Rev. Chem. Biomol. Eng.* 5, 301–323. <https://doi.org/10.1146/annurev-chembioeng-060713-040321>.
- Naidu, H., Mathews, A.P., 2021. Linear driving force analysis of adsorption dynamics in stratified fixed-bed adsorbers. *Sep. Purif. Technol.* 257 <https://doi.org/10.1016/j.seppur.2020.117955>.
- Nikulshina, V., Gálvez, M.E., Steinfeld, A., 2007. Kinetic analysis of the carbonation reactions for the capture of CO₂ from air via the Ca(OH)₂-CaCO₃-CaO solar thermochemical cycle. *Chem. Eng. J.* 129, 75–83. <https://doi.org/10.1016/j.cej.2006.11.003>.
- Ozkan, M., Nayak, S.P., Ruiz, A.D., Jiang, W., 2022. Current status and pillars of direct air capture technologies. *iScience* 25, 103990. <https://doi.org/10.1016/j.isci.2022.103990>.
- Patel, H.A., Hyun Je, S., Park, J., Chen, D.P., Jung, Y., Yavuz, C.T., Coskun, A., 2013. Unprecedented high-temperature CO₂ selectivity in N-2-phobic nanoporous covalent organic polymers. *Nat. Commun.* 4 <https://doi.org/10.1038/ncomms2359>.
- Pinsent, B.R.W., Pearson, L., Roughton, F.J.W., 1956. The kinetics of combination of carbon dioxide with hydroxide ions. *Trans. Faraday Soc.* 52, 1512–1520. <https://doi.org/10.1039/ft9565201512>.
- Planas, N., Dzubak, A.L., Poloni, R., Lin, L.C., McManus, A., McDonald, T.M., Neaton, J. B., Long, J.R., Smit, B., Gagliardi, L., 2013. The mechanism of carbon dioxide adsorption in an alkylamine-functionalized metal-organic framework. *J. Am. Chem. Soc.* 135, 7402–7405. <https://doi.org/10.1021/ja4004766>.
- Queen, W.L., Brown, C.M., Britt, D.K., Zajdel, P., Hudson, M.R., Yaghi, O.M., 2011. Site-specific CO₂ adsorption and zero thermal expansion in an anisotropic pore network. *J. Phys. Chem. C* 115, 24915–24919. <https://doi.org/10.1021/jp208529p>.
- Realf, M.J., Min, Y.J., Jones, C.W., Lively, R.P., 2021. Perspective - the need and prospects for negative emission technologies - direct air capture through the lens of current sorption process development. *Kor. J. Chem. Eng.* 38, 2375–2380. <https://doi.org/10.1007/s11814-021-0957-3>.
- Rodrigues, A.E., Silva, C.M., 2016. What's wrong with Lagergreen pseudo first order model for adsorption kinetics? *Chem. Eng. J.* 306, 1138–1142. <https://doi.org/10.1016/j.cej.2016.08.055>.

- Ryan, E.M., DeCroix, D., Breault, R., Xu, W., Huckaby, E.D., Saha, K., Dartevelle, S., Sun, X., 2013. Multi-phase CFD modeling of solid sorbent carbon capture system. *Powder Technol.* 242, 117–134. <https://doi.org/10.1016/j.powtec.2013.01.009>.
- Sabatino, F., Grimm, A., Gallucci, F., van Sint Annaland, M., Kramer, G.J., Gazzani, M., 2021. A comparative energy and costs assessment and optimization for direct air capture technologies. *Joule* 5, 2047–2076. <https://doi.org/10.1016/j.joule.2021.05.023>.
- Sadeghizadeh, A., Rahimi, R., Farhad Dad, F., 2018. Computational fluid dynamics modeling of carbon dioxide capture from air using biocatalyst in an airlift reactor. *Bioresour. Technol.* 253, 154–164. <https://doi.org/10.1016/j.biortech.2018.01.025>.
- Samari, M., Ridha, F., Manovic, V., Macchi, A., Anthony, E.J., 2019. Direct capture of carbon dioxide from air via lime-based sorbents. *Mitig. Adapt. Strategies Glob. Change* 25, 25–41. <https://doi.org/10.1007/s11027-019-9845-0>.
- Sandalow, D., Friedmann, J., McCormick, C., McCoy, S., 2018. *Direct Air Capture - ICEF Roadmap 2018. Direct Air Capture of Carbon Dioxide - ICEF Roadmap 2018*.
- Santori, G., Charalambous, C., Ferrari, M.C., Brandani, S., 2018. Adsorption artificial tree for atmospheric carbon dioxide capture, purification and compression. *Energy* 162, 1158–1168. <https://doi.org/10.1016/j.energy.2018.08.090>.
- Sanz-Pérez, E.S., Murdock, C.R., Didas, S.A., Jones, C.W., 2016. Direct capture of CO₂ from ambient air. *Chem. Rev.* 116, 11840–11876. <https://doi.org/10.1021/acs.chemrev.6b00173>.
- Schellevis, H.M., van Schagen, T.N., Brilman, D.W.F., 2021. Process optimization of a fixed bed reactor system for direct air capture. *Int. J. Greenh. Gas Control* 110. <https://doi.org/10.1016/j.ijggc.2021.103431>.
- Serna-Guerrero, R., Belmabkhout, Y., Sayari, A., 2010. Modeling CO₂ adsorption on amine-functionalized mesoporous silica: 1. A semi-empirical equilibrium model. *Chem. Eng. J.* 161, 173–181. <https://doi.org/10.1016/j.cej.2010.04.024>.
- Shi, X., Xiao, H., Liao, X., Armstrong, M., Chen, X., Lackner, K.S., 2018. Humidity effect on ion behaviors of moisture-driven CO₂ sorbents. *J. Chem. Phys.* 149. <https://doi.org/10.1063/1.5027105>.
- Shi, X., Xiao, H., Yonezu, A., Klaus, S., Chen, X., 2020. Moisture-driven CO₂ sorbents. *Joule* 4, 1823–1837. <https://doi.org/10.1016/j.joule.2020.07.00>.
- Sinha, A., Darunte, L.A., Jones, C.W., Realf, M.J., Kawajiri, Y., 2017. Systems design and economic analysis of direct air capture of CO₂ through temperature vacuum swing adsorption using MIL-101(Cr)-PEI-800 and mmen-Mg₂(dobpdc) MOF adsorbents. *Ind. Eng. Chem. Res.* 56, 750–764. <https://doi.org/10.1021/acs.iecr.6b03887>.
- Sinha, A., Thakkar, H., Rezaei, F., Kawajiri, Y., Realf, M.J., 2022. Reduced building energy consumption by combined indoor CO₂ and H₂O composition control. *Appl. Energy* 322, 119526. <https://doi.org/10.1016/j.apenergy.2022.119526>.
- Socolow, R., Desmond, M., Aines, R., Blackstock, J., Bolland, O., Kaarsberg, T., Lewis, N., Mazzotti, M., Pfeffer, A., Sawyer, K., Sirola, J., Smit, B., Wilcox, J., 2011. *Direct Air Capture of CO₂ with Chemicals A Technology Assessment for the APS Panel on Public Affairs. Technology (Singap World Sci)*, pp. 1–119.
- Stampi-Bombelli, V., van der Spek, M., Mazzotti, M., 2020. Analysis of direct capture of CO₂ from ambient air via steam-assisted temperature-vacuum swing adsorption. *Adsorption* 26, 1183–1197. <https://doi.org/10.1007/s10450-020-00249-w>.
- Sutanto, S., Dijkstra, J.W., Pieterse, J.A.Z., Boon, J., Hauwert, P., Brilman, D.W.F., 2017. CO₂ removal from biogas with supported amine sorbents: first technical evaluation based on experimental data. *Sep. Purif. Technol.* 184, 12–25. <https://doi.org/10.1016/j.seppur.2017.04.030>.
- Timmons, D., Terwel, R., 2022. Economics of aviation fuel decarbonization: a preliminary assessment. *J. Clean. Prod.* 369. <https://doi.org/10.1016/j.jclepro.2022.133097>.
- Tregambi, C., Bareschino, P., Hanak, D.P., Montagnaro, F., Pepe, F., Mancusi, E., 2022. Modelling of an integrated process for atmospheric carbon dioxide capture and methanation. *J. Clean. Prod.* 356. <https://doi.org/10.1016/j.jclepro.2022.131827>.
- Valentine, J., Zoelle, A., 2022. *Direct Air Capture Case Studies: Sorbent System (Pittsburg)*.
- Van Straelen, J., Geuzebroek, F., 2011. The thermodynamic minimum regeneration energy required for post-combustion CO₂ capture. In: *Energy Procedia*. Elsevier Ltd, pp. 1500–1507. <https://doi.org/10.1016/j.egypro.2011.02.017>.
- Veneman, R., Frigka, N., Zhao, W., Li, Z., Kersten, S., Brilman, W., 2015. Adsorption of H₂O and CO₂ on supported amine sorbents. *Int. J. Greenh. Gas Control* 41, 268–275. <https://doi.org/10.1016/j.ijggc.2015.07.014>.
- Vochozka, M., Horák, J., Krulický, T., Pardal, P., 2020. Predicting future brent oil price on global markets. *Acta Montan. Slovaca* 25, 375–392. <https://doi.org/10.46544/AMS.v25i3.10>.
- Wang, Y., LeVan, M.D., 2009. Adsorption equilibrium of carbon dioxide and water vapor on zeolites 5a and 13X and silica gel: pure components. *J. Chem. Eng. Data* 54, 2839–2844. <https://doi.org/10.1021/je800900a>.
- Wang, T., Lackner, K.S., Wright, A., 2011. Moisture swing sorbent for carbon dioxide capture from ambient air. *Environ. Sci. Technol.* 45, 6670–6675. <https://doi.org/10.1021/es201180v>.
- Wang, T., Liu, J., Fang, M., Luo, Z., 2013. A moisture swing sorbent for direct air capture of carbon dioxide: thermodynamic and kinetic analysis. *Energy Proc.* 37, 6096–6104. <https://doi.org/10.1016/j.egypro.2013.06.538>.
- Wang, T., Hou, C., Ge, K., Lackner, K.S., Shi, X., Liu, J., Fang, M., Luo, Z., 2017. Spontaneous cooling absorption of CO₂ by a polymeric ionic liquid for direct air capture. *J. Phys. Chem. Lett.* 8, 3986–3990. <https://doi.org/10.1021/acs.jpcc.7b01726>.
- Wang, H., Qu, Z.G., Bai, J.Q., Qiu, Y.S., 2018. Combined grand canonical Monte Carlo and finite volume method simulation method for investigation of direct air capture of low concentration CO₂ by 5A zeolite adsorbent bed. *Int. J. Heat Mass Tran.* 126, 1219–1235. <https://doi.org/10.1016/j.ijheatmasstransfer.2018.06.052>.
- Wang, H., Li, Z., Cai, N., 2020. Multiscale model for steam enhancement effect on the carbonation of CaO particle. *Chem. Eng. J.* 394, 124892. <https://doi.org/10.1016/j.cej.2020.124892>.
- Wang, Z., Goyal, N., Liu, L., Tsang, D.C.W., Shang, J., Liu, W., Li, G., 2020. N-doped porous carbon derived from polypyrrole for CO₂ capture from humid flue gases. *Chem. Eng. J.* 396, 125376. <https://doi.org/10.1016/j.cej.2020.125376>.
- Wang, R.L., Li, M.J., Li, D., Yang, Y.W., 2022. The synergy of light/fluid flow and membrane modification of a novel membrane microalgal photobioreactor for direct air carbon capture. *Appl. Energy* 328. <https://doi.org/10.1016/j.apenergy.2022.120133>.
- Wicaksana, A., 2016. IPCC, Global Warming of 1.5°C: Summary for Policy Makers, 2018. <https://medium.com/>.
- Wilcox, J., Rochana, P., Kirchofer, A., Glatz, G., He, J., 2014. Revisiting film theory to consider approaches for enhanced solvent-process design for carbon capture. *Energy Environ. Sci.* 7, 1769–1785. <https://doi.org/10.1039/c4ee00001c>.
- Wilson, S.M.W., Tezel, F.H., 2020. Direct dry air capture of CO₂ using VTSA with faujasite zeolites. *Ind. Eng. Chem. Res.* 59, 8783–8794. <https://doi.org/10.1021/acs.iecr.9b04803>.
- Wu, H., Simmons, J.M., Srinivas, G., Zhou, W., Yildirim, T., 2010. Adsorption sites and binding nature of CO₂ in prototypical metal-organic frameworks: a combined neutron diffraction and first-principles study. *J. Phys. Chem. Lett.* 1, 1946–1951. <https://doi.org/10.1021/jz100558r>.
- Wurzbacher, J.A., Gebald, C., Steinfeld, A., 2011. Separation of CO₂ from air by temperature-vacuum swing adsorption using diamine-functionalized silica gel. *Energy Environ. Sci.* 4, 3584–3592. <https://doi.org/10.1039/c1ee01681d>.
- Wurzbacher, J.A., Gebald, C., Piatkowski, N., Steinfeld, A., 2012. Concurrent separation of CO₂ and H₂O from air by a temperature-vacuum swing adsorption/desorption cycle. *Environ. Sci. Technol.* 46, 9191–9198.
- Wurzbacher, J.A., Gebald, C., Brunner, S., Steinfeld, A., 2016. Heat and mass transfer of temperature-vacuum swing desorption for CO₂ capture from air. *Chem. Eng. J.* 283, 1329–1338. <https://doi.org/10.1016/j.cej.2015.08.035>.
- Xiang, Z., Cao, D., Lan, J., Wang, W., Broom, D.P., 2010. Multiscale simulation and modelling of adsorptive processes for energy gas storage and carbon dioxide capture in porous coordination frameworks. *Energy Environ. Sci.* 3, 1469–1487. <https://doi.org/10.1039/c0ee00049c>.
- Xiao, G., Grace, J.R., Lim, C.J., 2014. Evolution of limestone particle size distribution in an air-jet attrition apparatus. *Ind. Eng. Chem. Res.* 53, 15845–15851. <https://doi.org/10.1021/ie501745h>.
- Xie, W.L., Chen, Z.J., Li, Z.Y., Tao, W.Q., 2016. Grand Canonical Monte Carlo simulation of nitrogen adsorption in a Silica aerogel model. *Computation* 4. <https://doi.org/10.3390/computation4020018>.
- Yang, K., Wu, J., Li, C., Xiang, Y., Yang, G., 2020. Efficient method to obtain the force field for CO₂ adsorption on zeolite 13X: understanding the host-guest interaction mechanisms of low-pressure adsorption. *J. Phys. Chem. C* 124, 544–556. <https://doi.org/10.1021/acs.jpcc.9b09187>.
- Yang, K., Yang, G., Wu, J., 2021a. Insights into the enhancement of CO₂ adsorption on faujasite with a low Si/Al ratio: understanding the formation sequence of adsorption complexes. *Chem. Eng. J.* 404, 127056. <https://doi.org/10.1016/j.cej.2020.127056>.
- Yang, K., Yang, G., Wu, J., 2021b. Quantitatively understanding the insights into CO₂ adsorption on faujasite from the heterogeneity and occupancy sequence of adsorption sites. *J. Phys. Chem. C* 125, 15676–15686. <https://doi.org/10.1021/acs.jpcc.1c04254>.
- Young, J., Garcia-Díez, E., Garcia, S., Van Der Spek, M., 2021. The impact of binary water-CO₂ isotherm models on the optimal performance of sorbent-based direct air capture processes. *Energy Environ. Sci.* 14, 5377–5394. <https://doi.org/10.1039/d1ee01272j>.
- Yun, J.H., He, Y., Otero, M., Düren, T., Seaton, N.A., 2002. Adsorption equilibrium of polar/non-polar mixtures on MCM-41: experiments and Monte Carlo simulation. *Stud. Surf. Sci. Catal.* 144, 685–692. [https://doi.org/10.1016/s0167-2991\(02\)80197-5](https://doi.org/10.1016/s0167-2991(02)80197-5).
- Zeman, F., 2008. Effect of steam hydration on performance of lime sorbent for CO₂ capture. *Int. J. Greenh. Gas Control* 2, 203–209. [https://doi.org/10.1016/S1750-5836\(07\)00115-6](https://doi.org/10.1016/S1750-5836(07)00115-6).
- Zhang, Z.X., Xu, H.J., Hua, W.S., Zhao, C.Y., 2022. Thermodynamics analysis of multi-stage temperature swing adsorption cycle for dilute CO₂ capture, enrichment and purification. *Energy Convers. Manag.* 265. <https://doi.org/10.1016/j.enconman.2022.115794>.
- Zhao, M., Xiao, J., Gao, W., Wang, Q., 2022. Defect-rich Mg-Al MMOs supported TEPA with enhanced charge transfer for highly efficient and stable direct air capture. *J. Energy Chem.* 68, 401–410. <https://doi.org/10.1016/j.jechem.2021.12.031>.
- Zhu, X., Ge, T., Yang, F., Wang, R., 2021a. Design of steam-assisted temperature vacuum-swing adsorption processes for efficient CO₂ capture from ambient air. *Renew. Sustain. Energy Rev.* 137, 110651. <https://doi.org/10.1016/j.rser.2020.110651>.
- Zhu, X., Lyu, M., Ge, T., Wu, J., Chen, C., Yang, F., O'Hare, D., Wang, R., 2021b. Modified layered double hydroxides for efficient and reversible carbon dioxide capture from air. *Cell Rep Phys Sci* 2, 100484. <https://doi.org/10.1016/j.xcrp.2021.100484>.